Research Square

Preprints are preliminary reports that have not undergone peer review.
They should not be considered conclusive, used to inform clinical practice,
or referenced by the media as validated information.

Toward Intelligent Thermal Fluids: AI-Driven Design of Zeta-Engineered Nanofluids and Self-Organized Thermal Transport Networks

Zhong Hu

zhong.hu@sdstate.edu

South Dakota State University

Haiping Hong

Iowa State University

Research Article

Keywords: Artificial intelligence, Nanofluids, Thermal management systems, Zeta-potential, Physics-informed machine learning, Multi-objective optimization, Thermal transport networks

Posted Date: November 4th, 2026

DOI: https://doi.org/10.21203/rs.3.rs-11352574/v1

License: This work is licensed under a Creative Commons Attribution 4.0 International License.
Read Full License

Additional Declarations: No competing interests reported.

Toward Intelligent Thermal Fluids: AI-Driven Design of Zeta-Engineered Nanofluids and Self-Organized Thermal Transport Networks

Zhong Hu [a*], and Haiping Hong[b]

[a] Department of Mechanical Engineering, South Dakota State University, Brookings, SD 57007, USA
[b] Department of Industrial & Manufacturing Systems Engineering, Iowa State University, Ames, IA 50011, USA; hhong@iastate.edu

[*] Correspondence: zhong.hu@sdstate.edu

Abstract: The development of next-generation nanofluids requires a shift from empirical formulation approaches toward data-driven design strategies that simultaneously optimize thermal conductivity, dynamic viscosity, stability, and system-level performance. This perspective highlights the emerging convergence of artificial intelligence (AI), zeta-potential (ZP) engineering, and advanced nanomaterials for the design of intelligent thermal fluids. Particular emphasis is placed on ZP-engineered nanofluids, in which electrostatic interactions are deliberately tailored to control nanoparticle dispersion, stability, and the formation of self-organized thermal transport networks. While interconnected nanoparticle networks can enhance thermal transport, excessive network connectivity, especially in high-aspect-ratio nanomaterials such as carbon nanotubes and graphene derivatives, may increase the dynamic viscosity and hydraulic resistance. Therefore, optimal nanofluid design requires balancing competing thermophysical and operational objectives under application-specific conditions. An AI-driven framework integrating machine learning, physics-informed machine learning, explainable AI, active learning, and multi-objective optimization is presented to accelerate nanofluid discovery and optimization. A representative case study of ZP-engineered iron oxide-carbon nanotube-graphene oxide nanofluids demonstrates the use of data-driven modeling, feature-importance analysis, SHAP interpretation, and Pareto optimization. The integration of AI-guided optimization with ZP-controlled network engineering provides a promising pathway toward intelligent thermal fluids and autonomous materials discovery for advanced thermal management systems.

Keywords: Artificial intelligence, Nanofluids, Thermal management systems, Zeta-potential, Physics-informed machine learning, Multi-objective optimization, Thermal transport networks

1. INTRODUCTION

The continuous increase in power density across modern technologies, including electric vehicles (EVs), data centers, power electronics, advanced energy systems, aerospace platforms, and defense systems, has intensified the demand for more efficient thermal management systems. Conventional heat-transfer fluids, such as water, ethylene glycol, propylene glycol, polyalphaolefin, and their mixtures, possess relatively low thermal conductivities, limiting their ability to dissipate increasingly high heat fluxes. Since the introduction of the nanofluid concept, dispersions of nanoscale particles within base fluids have been extensively investigated as potential high-performance coolants capable of enhancing heat transfer performance beyond that achievable with conventional fluids [1-3]. Reported

improvements in the thermal conductivity and convective heat transfer have stimulated significant research interest in nanofluids for thermal management applications.

Despite more than two decades of intensive research, widespread commercialization of nanofluids remains limited. While many nanofluid formulations exhibit enhanced thermal conductivities under laboratory conditions, practical deployment requires simultaneous improvements in colloidal stability, viscosity control, hydraulic efficiency, material compatibility, long-term reliability, manufacturing scalability, and economic viability [4-6]. These requirements introduce complex and frequently competing design objectives that cannot be addressed through the thermal conductivity enhancement alone. Consequently, the next generation of nanofluids will likely be defined not simply by the nanoparticle composition, but by the intelligent design of nanoparticle interactions, network architecture, and system-level thermophysical performance.

1.1 Challenges in Nanofluid Design

Nanofluid performance is governed by a wide range of interdependent physicochemical parameters. Nanoparticles investigated for thermal management applications generally include metal nanoparticles (Cu, Ag, Au), metal-oxide nanoparticles (Al_2O_3, CuO, TiO_2, Fe_3O_4), carbon-based nanomaterials (carbon nanotubes (CNTs), graphene nanoplatelets, graphene oxide (GO), reduced GO, nanodiamonds), and hybrid nanostructures combining multiple nanoparticle types [3,7,8]. Each nanoparticle class offers distinct advantages and limitations in terms of thermal conductivity, stability, cost, processability, and rheological behavior.

In addition to the nanoparticle composition, nanofluid performance is strongly influenced by the particle size, aspect ratio, concentration, surface chemistry, zeta potential (ZP), pH, ionic strength, base-fluid composition, synthesis route, and operating condition. These variables interact nonlinearly across multiple length scales, creating a high-dimensional design space that is difficult to explore by using conventional trial-and-error experimentation [3,9,10]. As a result, traditional empirical optimization approaches often require extensive experimental effort while yielding only limited understanding of the underlying structure-property relationships.

Among these parameters, the nanoparticle morphology plays a particularly important role because it directly influences network connectivity and transport behavior. Spherical nanoparticles primarily contribute through localized conduction and interfacial interactions, whereas high-aspect-ratio nanostructures such as CNTs and graphene derivatives can establish long-range conductive pathways within the fluid [11-13]. Numerous studies have shown that anisotropic nanomaterials generally achieve greater thermal conductivity enhancements at lower loadings than spherical particles. However, the increased network connectivity is often accompanied by a higher dynamic viscosity and a larger hydraulic resistance. Therefore, optimization of the nanoparticle morphology must consider both heat-transfer enhancement and flow-related penalties [14-16].

Another critical design variable is the ZP, which characterizes the electrokinetic state of nanoparticles within a suspension. Traditionally, ZP has been used as an indicator of colloidal stability because higher absolute ZP values strengthen electrostatic repulsion and suppress particle aggregation [17-19]. More recently, ZP has emerged as an active design parameter capable of regulating nanoparticle assembly, dispersion behavior, and network formation

[20-22]. Through controlled surface functionalization and electrostatic interactions, nanoparticles with complementary charge characteristics can be engineered to form stable and interconnected transport architectures while maintaining acceptable colloidal stability. This evolution from stability control to network engineering represents a significant shift in nanofluid design philosophy.

1.2 Thermal Transport and Stability Mechanisms

The mechanisms responsible for thermal conductivity enhancement in nanofluids remain an active area of investigation. Thermal transport is generally understood to arise from the combined effects of Brownian motions, interfacial transport phenomena, particle interactions, and network formations [23-25]. The relative contribution of each mechanism depends on the nanoparticle size, morphology, concentration, surface chemistry, and operating condition.

The Brownian motion has been proposed as one mechanism contributing to enhanced heat transfer. Random particle motions can induce microscopic mixing and energy exchange within the fluid, particularly for small nanoparticles and elevated temperatures. Although its quantitative contribution remains debated [24,26], The Brownian motion may influence local transport behavior and nanoparticle interactions. Interfacial transport mechanisms also play an important role. Ordered liquid layers formed around nanoparticles can modify local thermal transport characteristics and reduce interfacial resistance between solid and liquid phases [27,28].

Among the proposed mechanisms, percolation-based transport has emerged as one of the most compelling explanations for the exceptional performance reported in carbon-based and hybrid nanofluids. High-aspect-ratio nanostructures such as CNTs and GO nanosheets can form interconnected conductive pathways that facilitate long-range heat transport throughout the suspension [29-31]. However, network formation introduces an important trade-off. Although the increased network connectivity often improves the thermal conductivity, highly connected structures may simultaneously increase the fluid dynamic viscosity, pressure drop, and pumping-power requirement [16,32-34]. This effect is particularly pronounced in nanofluids containing elongated nanoparticles such as CNTs, nanofibers, and graphene-based structures. Consequently, the thermal conductivity enhancement and dynamic viscosity increase are governed by different physical mechanisms and do not necessarily scale proportionally. The optimal degree of network connectivity therefore depends strongly on application-specific operating conditions, including static versus dynamic applications and laminar versus turbulent flow regimes [16,33,34].

The challenge is thus not to maximize thermal conductivity alone, but to engineer nanoparticle networks that provide favorable thermal-hydraulic performance while preserving long-term stability. This perspective motivates the concept of ZP-engineered nanofluids, where controlled electrostatic interactions are used to regulate both network architecture and colloidal behavior [17,18,35].

1.3 AI-Driven Design Opportunity

The complexity of nanofluid systems presents a significant challenge for conventional analytical and empirical models. Classical theories, including effective-medium formulations and classical suspension models, often fail to accurately describe advanced hybrid nanofluids because they do not fully account for the electrostatic interaction,

network topology, percolation behavior, and multi-physics coupling [5,10,36]. Moreover, the large number of interacting design variables creates a vast formulation space that is impractical to explore experimentally.

Recent advances in artificial intelligence (AI), machine learning (ML), materials informatics, and physics-informed machine learning (PIML) provide new opportunities to transform nanofluid development from empirical experimentation to predictive design [37-39]. By learning nonlinear relationships directly from experimental, simulation, and literature-derived datasets, AI models can establish quantitative links between nanoparticle descriptors and macroscopic performance metrics. Parameters such as the nanoparticle composition, aspect ratio, concentration, ZP, pH, network density, and operating conditions can be incorporated into data-driven frameworks for predicting the thermal conductivity, dynamic viscosity, stability, pressure drop, and overall thermal management performance [39-41].

Particularly promising is the integration of AI-driven optimization with ZP engineering. In contrast to conventional nanofluids based on randomly dispersed particles, ZP-engineered systems intentionally manipulate electrostatic interactions to regulate nanoparticle assembly and network topology. ML frameworks can then be used to identify formulations that simultaneously improve thermal transport, limit viscosity increase, maintain colloidal stability, and satisfy application-specific constraints [40,42-44]. As a result, AI becomes not merely a prediction tool but an active enabler of intelligent thermal-fluid design.

1.4 Scope and Contributions of This Work

This article presents a perspective on the emerging convergence of AI, ZP engineering, and advanced nanomaterials for the development of intelligent thermal fluids [37,39,45]. Rather than providing a comprehensive review of nanofluids, the focus is placed on design principles that enable the rational engineering of thermally conductive and colloidally stable nanoparticle networks. Particular attention is given to the role of ZP as a controllable design parameter, the importance of network architecture in governing thermal-hydraulic performance, and the application of AI-driven methodologies for accelerated formulation development.

The article first summarizes the physical foundations of ZP-engineered nanofluids and the mechanisms governing thermal transport, stability, and performance trade-offs. Subsequently, an AI-driven design framework is presented that integrates ML, explainable AI (XAI), PIML, active learning, and multi-objective optimization (MOO). A representative case study involving ZP-engineered Fe_3O_4-CNT-GO nanofluids is then used to demonstrate literature-derived database development, surrogate modeling, feature-importance analysis, Shapley Additive explanation (SHAP) interpretation, and Pareto-based optimization. Finally, current challenges and future opportunities are discussed, with particular emphasis on autonomous materials discovery, digital twins, adaptive thermal fluids, and intelligent thermal management systems [43,40,46,47]. The objective of overarching is to establish a research-guidance framework for AI-enabled design of ZP-engineered nanofluids and to outline a pathway toward next-generation intelligent thermal fluids.

Figure 1 illustrates the proposed AI-driven nanofluid design framework, which integrates nanoparticle descriptors, ML, physics-informed modeling, XAI, and MOO to accelerate the discovery of high-performance

nanofluids. The approach enables simultaneous optimization of thermal conductivity, dynamic viscosity, stability, and hydraulic performance, providing a pathway toward intelligent thermal fluids and application-specific thermal management solutions.

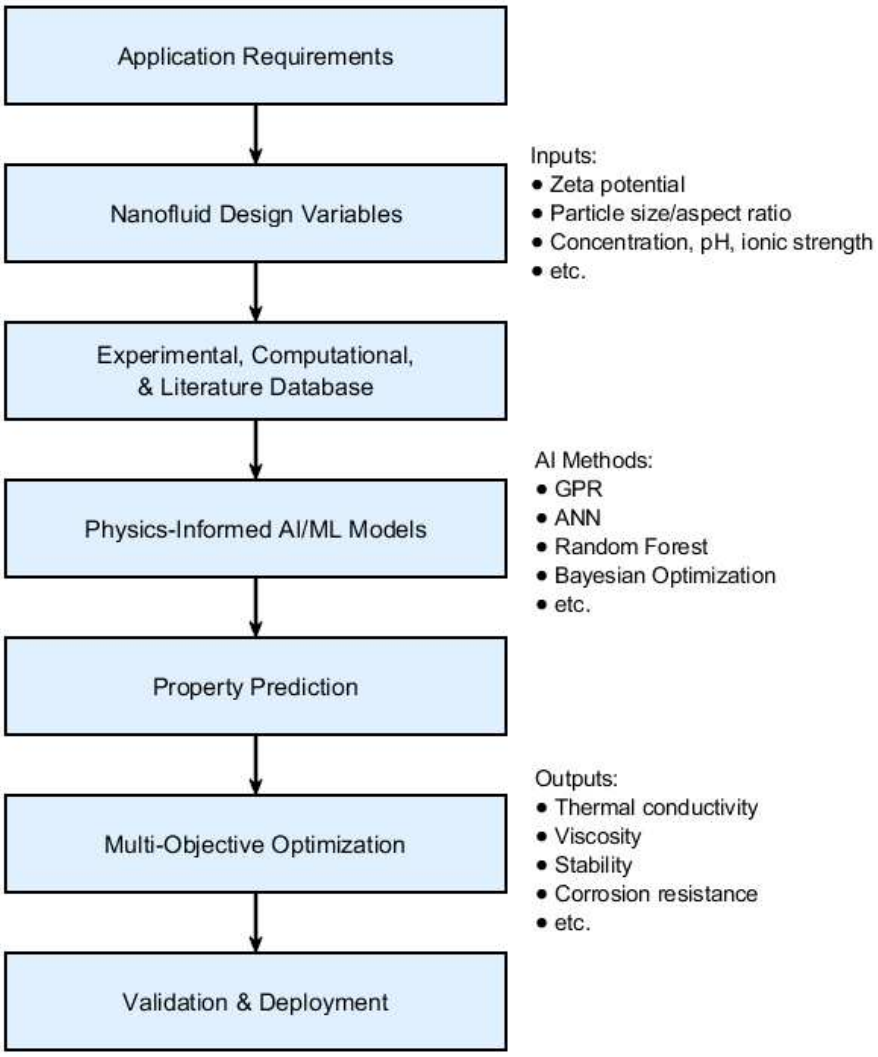


Figure 1: Schematic framework of AI-driven nanofluid design and optimization.

2. PHYSICAL FOUNDATIONS OF ZETA-ENGINEERED NANOFLUIDS

The development of intelligent thermal fluids requires a fundamental understanding of the coupled relationships among colloidal interactions, thermal transport pathways, rheological behavior, and system-level performance. Unlike conventional nanofluids, which often rely on randomly dispersed nanoparticles, ZP-engineered nanofluids are intentionally designed to exploit electrostatic interactions and controlled nanoparticle assembly. The objective is not merely to enhance thermal conductivity, but to achieve a favorable balance among the thermal transport, dynamic viscosity, stability, pressure drop, and manufacturability. Consequently, nanofluid design evolves from

simple particle dispersion toward the engineering of functional transport networks governed by both physical principles and data-driven optimization.

2.1 Zeta-Potential Engineering and Self-Organized Thermal Transport Networks

Long-term colloidal stability remains one of the most critical requirements for practical nanofluid deployment. Nanofluids exhibiting even excellent thermal conductivity enhancements become unsuitable for industrial applications if aggregation, sedimentation, or network degradation occur during operation. Traditionally, colloidal stabilization has been achieved by maximizing electrostatic repulsion among dispersed nanoparticles through control of surface charge, pH, ionic strength, and surface functionalization [17-19].

In recent years, the role of ZP has expanded beyond its traditional function as a stability indicator. Rather than simply preventing particle interactions, ZP can be employed as an active design variable to regulate nanoparticle organization and network formation. Through appropriate surface functionalization and electrostatic tuning, nanoparticles possessing complementary charge characteristics can interact in a controlled manner, creating interconnected architectures while maintaining overall colloidal stability [20-22,48-50].

A representative example involves positively charged Fe_3O_4 nanoparticles combined with negatively charged CNTs and GO nanosheets. Electrostatic attraction promotes the formation of multidimensional nanoparticle assemblies consisting of:

- 0D Fe_3O_4 nanoparticles acting as thermal nodes,
- 1D CNTs serving as conductive bridges,
- 2D GO nanosheets functioning as thermal spreading platforms.

The resulting self-organized thermal transport networks (SOTTNs) provide an enhanced transport connectivity compared with randomly dispersed systems while preserving suspension stability through controlled interparticle interactions [20,21,35,48,51].

From an AI-driven design perspective, ZP, surface chemistry, nanoparticle dimensionality, and network descriptors become quantitative variables that can be optimized simultaneously with thermophysical properties. Consequently, ZP engineering represents a transition from passive stabilization toward active network engineering.

Figure 2 shows a schematic illustration of dispersion stability and ZP engineering for AI-enabled nanofluids. Electrostatic interactions among positively charged Fe_3O_4 nanoparticles and negatively charged CNTs/GO nanosheets create stable multidimensional thermal networks while suppressing aggregation and sedimentation.

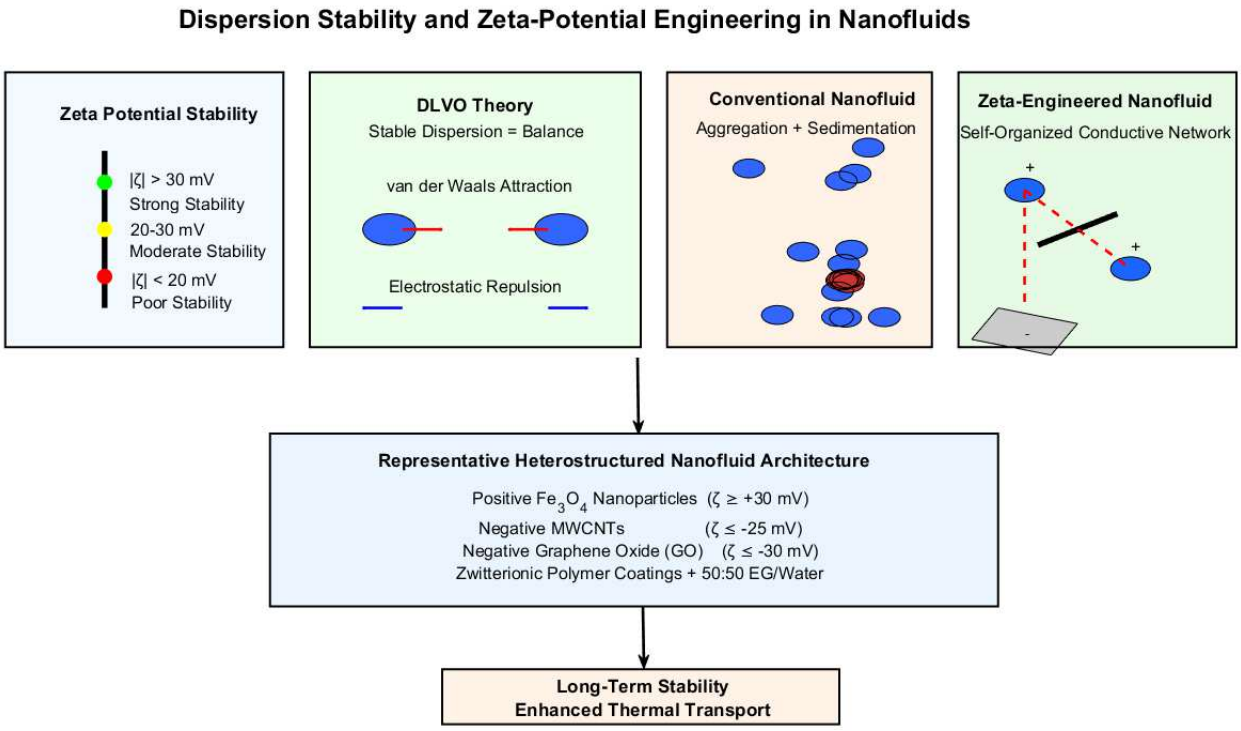


Figure 2: Schematic illustration of dispersion stability and ZP engineering nanofluids.

2.2 Percolation-Based Thermal Transport and Network Connectivity

Thermal conductivity enhancements in advanced hybrid nanofluids frequently exceed predictions obtained using classical effective-medium theories such as the Maxwell and Bruggeman models. These traditional approaches assume isolated particles dispersed within a continuous fluid phase and therefore do not adequately capture interparticle interactions and network effects [52-54].

Increasing evidences suggest that thermal transport in carbon-based and hybrid nanofluids is governed primarily by percolation-based transport mechanisms. According to the percolation theory, once conductive nanoparticles become sufficiently interconnected, a continuous thermal transport network is established throughout the suspension. After the percolation threshold is exceeded, heat propagation occurs preferentially through interconnected nanoparticle pathways rather than through the low-conductivity base fluid [29-31].

The effectiveness of such networks depends strongly on the nanoparticle dimensionality and connectivity. CNTs form long-range conductive bridges because of their high aspect ratios and exceptional intrinsic thermal conductivity [11,12,14]. Similarly, graphene and GO nanosheets provide multidirectional heat-spreading pathways with large interfacial contact areas [13,55]. When integrated into hybrid architectures, these materials establish hierarchical conductive networks that reduce interfacial thermal resistance and facilitate long-range phonon transport [28-30,56-58].

Importantly, the thermal conductivity enhancement is governed not only by nanoparticle loading but also by the network topology, node connectivity, contact density, and percolation efficiency. Consequently, the network

architecture becomes a more meaningful design variable than nanoparticle concentration alone. This perspective is particularly relevant for AI-guided optimization because network descriptors can be incorporated directly into ML models and optimization frameworks.

2.3 Performance Trade-Offs and System-Level Design Constraints

A major obstacle to widespread nanofluid implementation is the existence of competing thermophysical and operational requirements. While the conductivity enhancement remains an important objective, practical thermal-management applications require simultaneous consideration of dynamic viscosity, stability, pressure drop, corrosion, cost, and long-term reliability [4,8,36].

One of the most fundamental trade-offs involves thermal conductivity and dynamic viscosity. Increased nanoparticle loading generally improves thermal transport by increasing conductive pathways. However, higher particle concentrations also increase the effective dynamic viscosity, leading to larger pressure drops and greater pumping-power requirements. This challenge becomes particularly significant in nanofluids containing high-aspect-ratio nanoparticles such as CNTs and graphene derivatives [16,33,34].

A similar trade-off exists for network formation. Although interconnected nanoparticle networks can substantially improve thermal conductivity through percolation transport, highly connected structures often increase hydrodynamic resistance because the network impedes fluid motion. Consequently, the thermal conductivity enhancement and dynamic viscosity increase arise from different physical mechanisms and should not be assumed to scale proportionally. The optimal degree of the network connectivity is therefore strongly dependent on application conditions, including static versus dynamic systems and laminar versus turbulent flow environments [32-34].

From an engineering perspective, the most meaningful metric is not the maximum thermal conductivity but the maximum system-level thermal-hydraulic performance. For example, battery cooling systems may prioritize the thermal conductivity enhancement coupled with low pumping power, whereas thermal energy storage applications may tolerate a higher dynamic viscosity in exchange for superior heat transport. Similarly, aerospace and data-center cooling applications may impose additional constraints related to reliability, durability, and cost.

These competing objectives motivate the adoption of AI-driven MOO frameworks capable of identifying operating regions that balance the thermal performance, hydraulic efficiency, stability, and manufacturability simultaneously. Such considerations establish the physical foundation for the AI-enabled methodologies discussed in the following section.

Figure 3 shows a schematic illustration of application-dependent thermal-hydraulic trade-offs in nanofluid design and the role of AI-driven MOO. Improving one performance metric often negatively impacts another, necessitating simultaneous optimization of the thermal conductivity (k), dynamic viscosity (μ), stability, cost, etc.

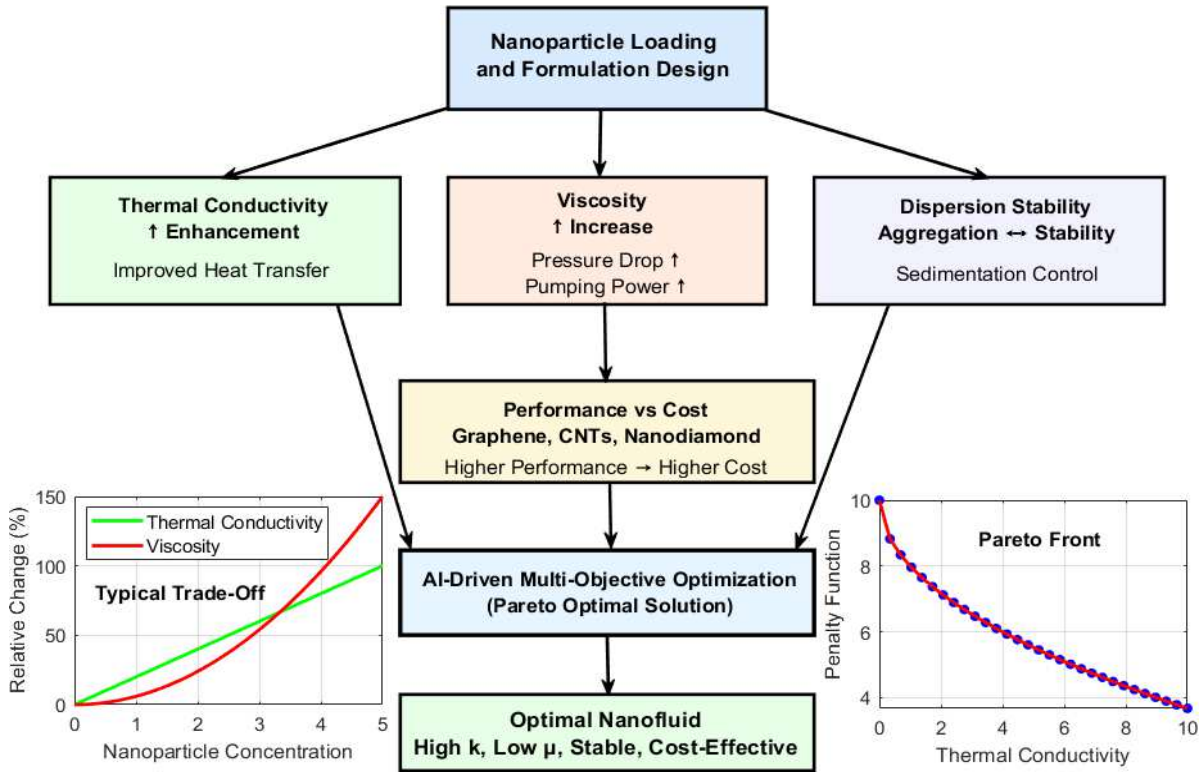


Figure 3: Schematic illustration of application-dependent thermal-hydraulic trade-offs in nanofluid design.

3. AI-DRIVEN DESIGN OF ZETA-ENGINEERED INTELLIGENT THERMAL FLUIDS

The development of intelligent thermal fluids requires the integration of colloidal engineering, thermal transport physics, and data-driven materials design. Unlike conventional nanofluid development, which relies heavily on empirical experimentation and iterative formulation adjustment, modern AI provides opportunities to establish predictive relationships between nanoparticle descriptors and system-level performance metrics. Recent advances in AI/ML, PIML, XAI, active learning, and MOO are transforming nanofluid development from trial-and-error experimentation toward rational and accelerated materials discovery.

Within this framework, ZP-engineered nanofluids represent an attractive design platform because colloidal stability, network formation, rheological behavior, and thermal transport can all be treated as interconnected optimization variables. By combining electrostatic control with AI-guided design strategies, it becomes possible to optimize not only nanoparticle composition but also nanoparticle interactions and transport-network architecture. Consequently, AI-enabled ZP-engineered nanofluids provide a promising pathway toward intelligent thermal fluids capable of simultaneously satisfying thermal conductivity, stability, dynamic viscosity, cost, and scalability requirements.

3.1 AI Framework for Nanofluid Design and Optimization

Nanofluid development involves a highly multidimensional design space composed of interacting

physicochemical variables, including the nanoparticle composition, particle morphology, concentration, surface chemistry, ZP, pH, ionic strength, base-fluid characteristics, and operating conditions. These variables collectively govern thermal conductivity, dynamic viscosity, stability, pressure drop, corrosion behavior, and overall system performance. Because of the strong nonlinear coupling among these parameters, traditional empirical correlations and one-factor-at-a-time experimental approaches often fail to efficiently identify optimal formulations [37-39].

A typical AI-driven nanofluid design workflow consists of five interconnected stages:

- Database development;
- Feature engineering;
- Surrogate-model construction;
- Explainable-AI analysis;
- Multi-objective optimization and validation.

The process begins with the construction of a comprehensive database consisting of thermophysical, rheological, and stability data extracted from the literature either experimentally measured or computationally simulated. Feature engineering subsequently converts raw experimental information into quantitative descriptors suitable for machine-learning analysis. Typical descriptors include the nanoparticle concentration, aspect ratio, particle size, ZP, network density, fractal dimension, interfacial area density, pH, temperature, and base-fluid composition.

ML models are then trained to establish relationships between these descriptors and target properties. Among the most widely used algorithms in nanofluid research are artificial neural networks (ANNs), support vector machines (SVMs), random forests (RFs), Gaussian process regression (GPR), gradient-boosting algorithms, and deep-learning architectures [37-39,59-62].

Particular interest has recently focused on RF and GPR models because they provide both high predictive accuracy and a degree of model interpretability. RF models are well suited for strongly nonlinear multivariable systems and provide feature-importance rankings, whereas GPR models offer probabilistic predictions and uncertainty quantification. These characteristics are particularly attractive for nanofluid design because experimental data often remain sparse and expensive to obtain [42,63-65].

After model training and validation, predictive surrogate models are integrated with optimization algorithms to guide formulation screening and candidate selection. Figure 4 illustrates the overall AI-driven nanofluid design workflow. By integrating experimental data, physical descriptors, predictive modeling, active learning, and optimization within a unified framework, AI significantly reduces experimental burden while accelerating formulation discovery.

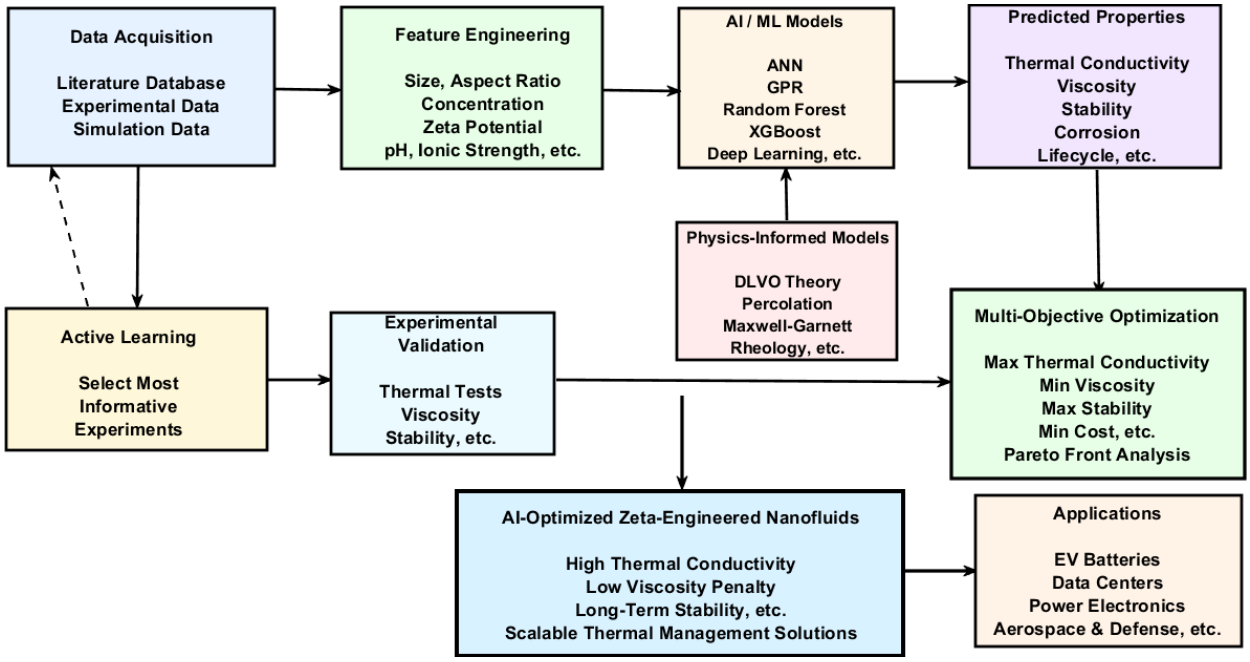


Figure 4: Summary workflow of AI-driven nanofluid design and optimization

3.2 Physics-Informed and Explainable AI for Nanofluid Engineering

Although purely data-driven models have demonstrated remarkable predictive capability, their extrapolation performance and physical interpretability often remain limited. High prediction accuracy alone does not necessarily provide scientific understanding of the transport mechanisms governing nanofluid behavior. Consequently, growing attention has been directed toward PIML frameworks and XAI methodologies [41,66,67].

PIML combines experimental data with established physical theories, enabling machine-learning models to satisfy known physical constraints while retaining predictive flexibility. For ZP-engineered nanofluids, relevant physical models include:

- DLVO theory for colloidal stability [68,69];
- Percolation theory for thermal-network formation [29,30];
- Effective-medium theories for thermal conductivity [52-54];
- Suspension rheology models for dynamic viscosity prediction [36].

The integration of these physical principles reduces overfitting, improves extrapolation capability, and increases confidence in AI-generated predictions. This capability is particularly important for nanofluids because experimentally accessible regions often represent only a small fraction of the overall formulation space.

Figure 5 schematically illustrates a PIML framework for nanofluid design and optimization. The figure illustrates how nanoparticle descriptors and physicochemical parameters serve as inputs to AI/ML models, which are integrated with transport physics and colloidal theories to predict and optimize nanofluid performance metrics including thermal conductivity (k), dynamic viscosity (μ), stability, corrosion resistance, and lifecycle performance.

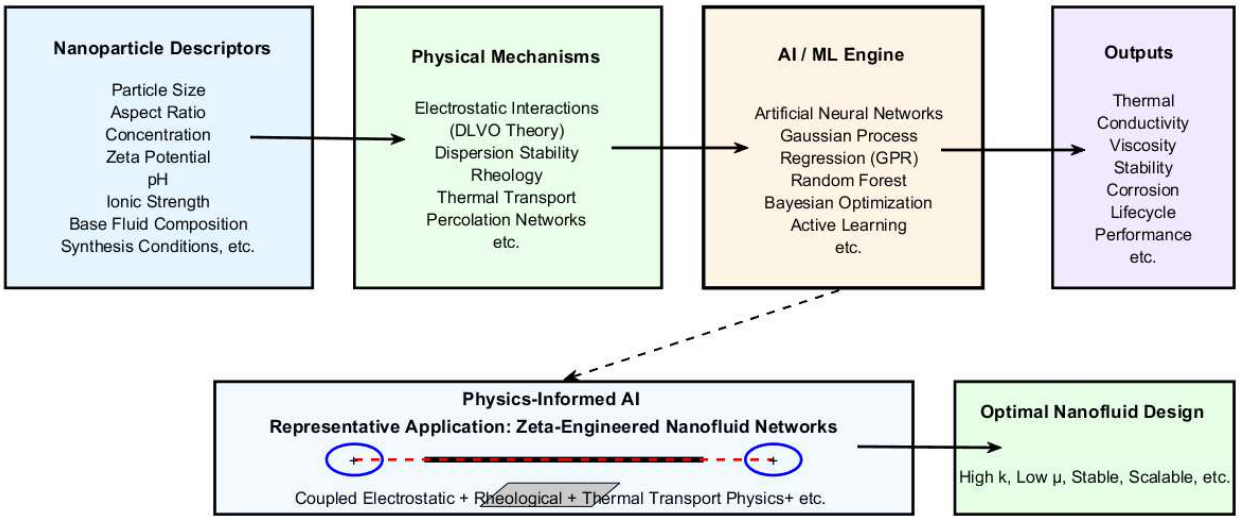


Figure 5: PIML framework for nanofluid design and optimization.

Complementing PIML, XAI techniques provide mechanistic insights into model predictions. Traditional black-box models frequently offer limited explanation regarding why specific inputs influence target properties. XAI addresses this challenge by quantifying the relative importance of individual descriptors and their contributions to model outputs.

Among the available approaches, feature-importance analysis and SHAP analysis are particularly useful for nanofluid research. Feature-importance methods identify globally influential design variables, whereas SHAP analyses provide both global and local interpretability, allowing researchers to understand how individual variables contribute to specific predictions [70].

For ZP-engineered nanofluids, XAI analyses consistently indicate that the nanoparticle composition, ZP, aspect ratio, network density, and fractal characteristics are among the dominant factors influencing the thermal conductivity, stability, dynamic viscosity, and pressure-drop behavior. Such findings suggest that nanofluid performance depends more strongly on nanoparticle interactions and transport-network architectures than on nanoparticle concentration alone.

Consequently, the combination of PIML and XAI provides a powerful framework for transforming nanofluid design from empirical optimization toward physically interpretable and scientifically guided materials engineering.

3.3 AI-Guided Multi-Objective Optimization of Zeta-Engineered Nanofluids

The practical implementation of nanofluids requires balancing multiple competing objectives rather than maximizing thermal conductivity alone. While enhanced thermal transport remains the primary motivation for nanofluid development, industrial applications simultaneously demand low dynamic viscosity, minimal pressure-drop penalty, long-term stability, corrosion resistance, manufacturability, and economic viability. Consequently, nanofluid design represents a highly constrained MOO problem in which improvements in one property frequently lead to degradation in another [33,40,43,71,72].

A prominent example is the conductivity-viscosity trade-off. Increasing the nanoparticle concentration generally improves thermal conductivity by increasing the density of conductive pathways. However, higher particle loading also increases dynamic viscosity, pressure drop, and pumping-power requirement. Similarly, the formation of interconnected thermal transport networks may enhance heat transfer efficiency but can simultaneously increase hydrodynamic resistance, particularly in nanofluids containing high-aspect-ratio nanomaterials such as CNTs and graphene derivatives [32-34,73]. Consequently, the optimal nanofluid formulation is highly application dependent and cannot be determined solely from thermal conductivity measurements.

AI-driven optimization provides a powerful framework for addressing these challenges. By coupling predictive surrogate models with intelligent search algorithms, large formulation spaces can be explored efficiently without the need for exhaustive experimentation. Common optimization approaches include genetic algorithms, Bayesian optimization, particle swarm optimization, evolutionary algorithms, and Pareto-front analysis [40,43,71,72]. Among these methods, the Non-Dominated Sorting Genetic Algorithm II (NSGA-II) has become one of the most widely adopted approaches because of its ability to identify diverse Pareto-optimal solutions while simultaneously handling multiple conflicting objectives [71,74].

For ZP-engineered nanofluids, MOO can be used to optimize a range of design variables, including the nanoparticle concentration, aspect ratio, ZP, network density, surface functionalization, and base-fluid composition. Typical optimization objectives include:

- maximizing thermal conductivity;
- maximizing colloidal stability;
- minimizing dynamic viscosity increase;
- minimizing pressure drop;
- minimizing corrosion risk;
- minimizing material cost.

Unlike traditional optimization strategies based on the nanoparticle loading alone, AI-guided approaches enable the simultaneous optimization of network topology and electrostatic interactions. As a result, nanoparticle connectivity, percolation efficiency, and thermal-hydraulic performance can be optimized concurrently within a unified design framework [37,41-43].

As AI methodologies continue to mature, optimization is expected to evolve toward adaptive and closed-loop design environments that integrate predictive modeling, active learning, automated experimentation, and real-time performance feedback. Such capabilities will accelerate the development of application-specific intelligent thermal fluids tailored for EV battery cooling, data-center liquid cooling, aerospace thermal control, and advanced energy systems, etc.

Figure 6 illustrates the proposed AI-driven framework for the rational design and optimization of ZP-engineered nanofluids. The workflow begins with nanoparticle and formulation descriptors, including, as an example, Fe_3O_4, CNT, and GO loadings, zeta potential, aspect ratio, network density, pH, and operating temperature. Through ZP engineering and polymer functionalization, oppositely charged nanoparticles are assembled into SOTTNs that

enhance network connectivity and percolation-based heat transport. Experimental characterization data are subsequently integrated with a physics-informed framework incorporating the DLVO theory, percolation theory, effective-medium theory, and suspension rheology. These physical principles are coupled with machine-learning models, including RF, GPR, SHAP/XAI, active learning, and NSGA-II optimization, to establish predictive relationships between nanofluid descriptors and performance metrics. The framework enables simultaneous optimization of thermal conductivity, dynamic viscosity, stability, pressure drop, and cost, generating Pareto-optimal solutions tailored to specific thermal-management applications.

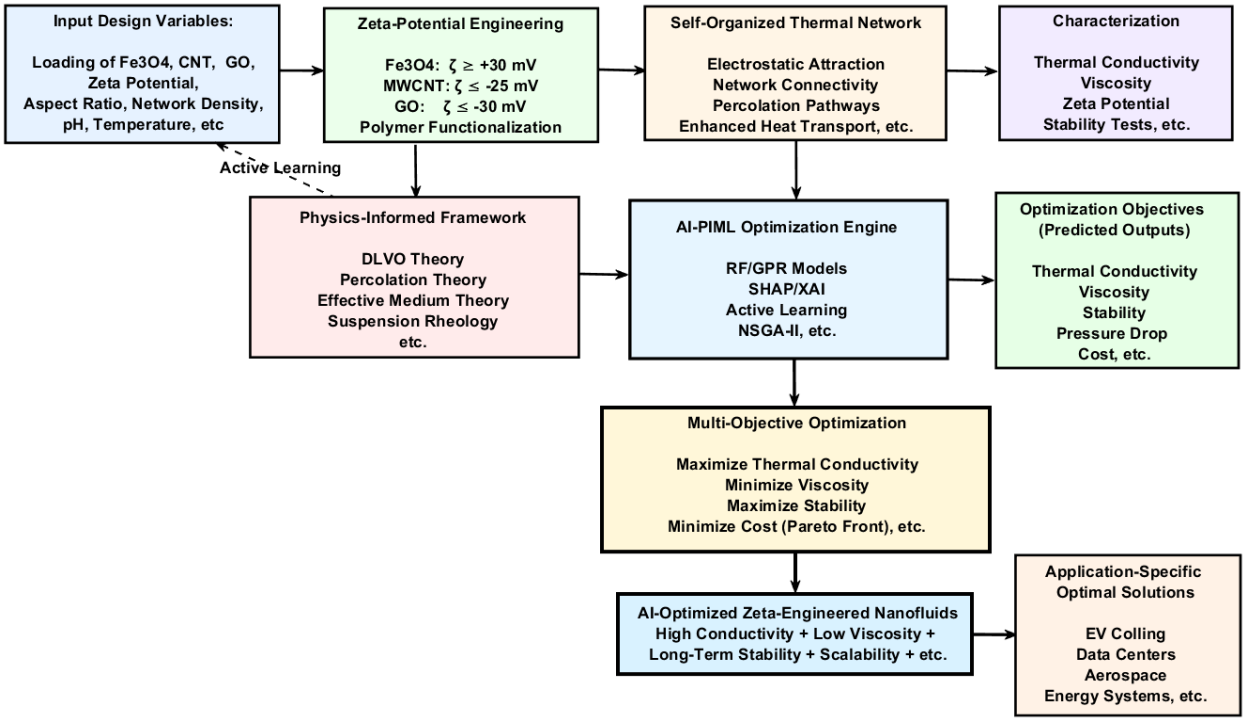


Figure 6. Application-Dependent Multi-Objective Optimization Framework for Intelligent Thermal Fluids.

3.4 Comparative Positioning of Emerging Nanofluid Technologies

Over the past two decades, nanofluid technologies have evolved from simple nanoparticle dispersions toward increasingly sophisticated and intelligent thermal-fluid systems. Early studies primarily focused on single-component nanofluids composed of metal or metal-oxide nanoparticles dispersed within conventional base fluids. While these formulations demonstrated measurable thermal conductivity enhancements, widespread adoption has been limited due to aggregation, sedimentation, and insufficient long-term reliability [3,4,7].

Subsequent advances introduced carbon-based nanofluids containing CNTs, graphene, GO, and related materials. Owing to their exceptionally high intrinsic thermal conductivity and favorable aspect ratios, these nanomaterials often produced significantly larger conductivity enhancements than traditional nanoparticles. However, strong van der Waals interactions frequently resulted in agglomeration and dynamic viscosity increases,

creating additional challenges for practical deployment [11-14,23,36,55].

The development of hybrid nanofluids represented an important step toward overcoming these limitations. By combining nanoparticles with complementary properties, hybrid systems exploit synergistic effects that improve thermal transport, dispersion stability, and thermal-hydraulic performance compared with single-component formulations [8,16,30]. More recently, AI-assisted formulation design has further accelerated nanofluid research by enabling predictive property modeling and optimization using literature-derived and experimental datasets [37-39,45,59-62,75].

The next stage of development is represented by AI-enabled ZP-engineered nanofluids. Unlike conventional approaches that primarily focus on the nanoparticle loading, these systems intentionally manipulate electrostatic interactions and nanoparticle-network architectures to optimize thermal transport pathways while preserving colloidal stability. Through the integration of ZP engineering, SOTTNs, PIML, and MOO, these formulations seek to simultaneously improve thermal conductivity, stability, and hydraulic efficiency [17-21,48].

Table 1 compares the characteristics of current and emerging nanofluid technologies. The comparison suggests a gradual transition from passive nanoparticle dispersions toward intelligent thermal-fluid platforms capable of predictive design and adaptive optimization [40,43].

Table 1. Comparison of key performance metrics of current and emerging nanofluid technologies.

Technology	Thermal Conductivity Enhancement	Stability	Viscosity Impact	Predictive Design Capability	Commercial Readiness	Major Limitations
Metal Nanoparticle Nanofluids (Cu, Ag, Au)	Moderate (15-35%)	Poor-Moderate	Moderate	Low	Low	Oxidation, cost, sedimentation
Metal Oxide Nanoparticle Nanofluids (Al_2O_3, CuO, TiO_2, Fe_3O_4)	Moderate (10-25%)	Moderate	Low-Moderate	Low	Medium	Aggregation, sedimentation, limited conductivity enhancement
CNT-Based Nanofluids	High (20-50%)	Poor	High	Low	Low	Agglomeration and viscosity increase
Graphene-Based Nanofluids	High (20-60%)	Moderate	Moderate-High	Low	Medium	Cost and dispersion challenges
Hybrid Nanofluids (CNT-GO, Fe_3O_4-Graphene, Al_2O_3-CuO)	High (25-50%)	Moderate-High	Moderate	Moderate	Medium	Increased formulation complexity and reproducibility challenges
AI-Optimized Conventional Nanofluids	High (25-50%)	Moderate-High	Moderate	High	Medium-High	Limited by conventional nanoparticle architectures and available datasets
AI-Enabled ZP-Engineered Nanofluids	Very High (25-50% currently; >50% projected)	High	Low-Moderate (<15%)	Very High	Emerging	Dataset standardization, manufacturing scale-up, technology maturity

Table 2 shows the technology comparison based on the critical performance metrics. This assessment suggests that AI-enabled ZP-engineered nanofluid systems are uniquely positioned to overcome the traditional conductivity-

stability-viscosity trade-off that has historically constrained commercialization by offering the most balanced approach among competing objectives.

Table 2. Technological trade-off comparison based on critical performance metrics.

Metric	Conventional Nanofluids	Hybrid Nanofluids	ZP-Engineered Nanofluids	AI-Enabled ZP-Engineered Nanofluids
Thermal Conductivity	Medium	High	High	Very High
Dispersion Stability	Low-Medium	Medium-High	High	Very High
Viscosity Control	Medium	Medium	High	High
Corrosion Management	Low	Medium	High	High
Predictability	Low	Medium	High	Very High
MOO	No	Limited	Yes	Yes
Scalability Potential	Medium	Medium	Medium-High	High
Industrial Suitability	Moderate	Good	Very Good	Excellent (Projected)

Important Note. The projected capabilities assigned to AI-enabled ZP-engineered nanofluids are based on emerging advances in hybrid nanofluids, electrostatic self-assembly, ML-assisted materials design, and SOTTNs [39,40,58-65]. Although encouraging progress has been reported, these systems remain at an early stage of technological development, and large-scale industrial validation has not yet been achieved. Therefore, the projected advantages should be interpreted as future potential rather than established commercial performance.

Figure 7 illustrates the progression from conventional nanoparticle dispersions to future AI-enabled ZP-engineered nanofluids. Early generations primarily relied on increasing the nanoparticle loading to enhance thermal conductivity, often at the expense of stability and hydraulic performance. Subsequent developments introduced carbon-based and hybrid nanofluids to exploit synergistic transport mechanisms and improved network connectivity. More recently, ML and materials informatics have enabled predictive formulation design and optimization. The emerging generation of AI-enabled ZP-engineered nanofluids combines electrostatic self-assembly, SOTTNs, PIML, and MOO to simultaneously improve thermal transport, colloidal stability, predictability, and application-specific thermal-hydraulic performance.

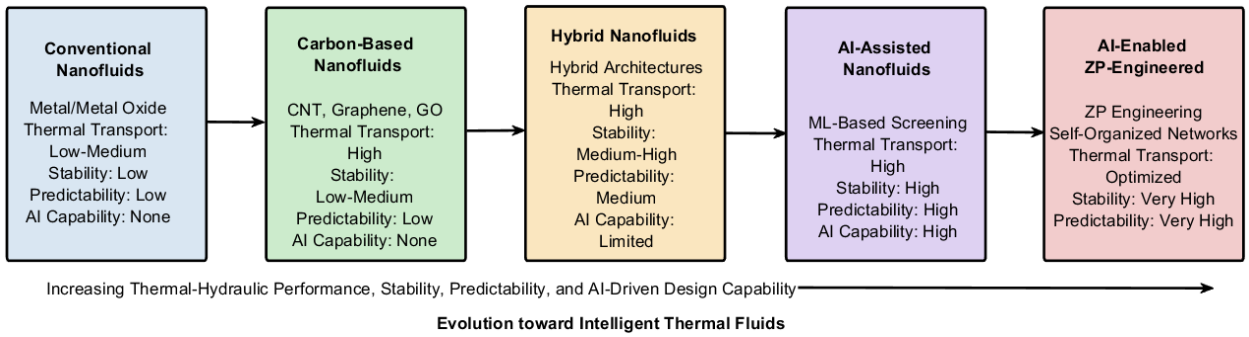


Figure 7. Evolution of nanofluid technologies toward intelligent thermal fluids.

3.5 Commercialization Challenges and Future Research Opportunities

Despite substantial scientific progress, several critical barriers continue to hinder the large-scale deployment of nanofluids in industrial thermal-management applications. These challenges extend beyond thermal conductivity enhancements and increasingly involve long-term reliability, reproducibility, manufacturability, and system-level performance [4,6,8].

- **Long-Term Stability and Network Durability**

Long-term stability remains the most significant challenge for practical nanofluid deployment. Agglomeration, sedimentation, and network degradation can progressively reduce thermal performance while increasing fouling and flow resistance. Carbon-based nanomaterials are particularly susceptible to aggregation due to strong van der Waals attractions. Future improvements are expected to arise from ZP engineering, surface functionalization, zwitterionic coatings, and AI-assisted degradation prediction models capable of forecasting long-term stability under realistic operating conditions [9,10,18,27,76,77].

- **Breaking the Thermal Conductivity-Viscosity Trade-Off**

The conductivity-viscosity trade-off continues to represent a fundamental scientific and engineering challenge. While percolation-based transport networks can substantially enhance thermal conductivity, excessive network connectivity often increases dynamic viscosity and hydraulic losses. Future design strategies should therefore focus on optimizing network architecture rather than maximizing the nanoparticle loading. AI-guided optimization and physics-informed rheological models offer promising opportunities for simultaneously improving heat-transfer performance and hydraulic efficiency [33,34,36,73].

- **Data Infrastructure and Standardization**

The effectiveness of AI-driven materials discovery depends strongly on the availability of large, high-quality datasets. However, current nanofluid databases remain fragmented because of inconsistent experimental methodologies, incomplete metadata reporting, and limited accessibility of negative results. The development of standardized nanofluid databases and community-wide reporting protocols will be essential for improving model robustness and reproducibility [44,78].

- **Explainable and Physics-Informed AI**

Although ML models frequently achieve excellent predictive accuracy, many remain difficult to interpret and are prone to extrapolation errors beyond the training domain. Future efforts should increasingly integrate PIML and XAI methodologies to improve interpretability, reliability, and scientific understanding. Such approaches can establish stronger connections between machine-learning predictions and underlying transport physics, thereby increasing confidence in AI-assisted formulation recommendations [41,66,67].

- **Digital Manufacturing and Digital Twins**

Commercial adoption will require scalable manufacturing processes capable of maintaining consistent quality and performance. AI-assisted process control, digital manufacturing, and digital-twin technologies offer

opportunities to establish process-property-performance relationships and improve production reproducibility. Coupling real-time monitoring with digital twins may further enable predictive quality control and adaptive manufacturing strategies [46,47].

- **Autonomous Materials Discovery**

One of the most promising future directions is the emergence of autonomous materials discovery platforms integrating active learning, robotic experimentation, automated characterization, and AI-driven optimization. Such systems can iteratively design experiments, update predictive models, and explore formulation spaces with minimal human intervention. The convergence of AI, automation, and materials informatics has the potential to dramatically accelerate nanofluid development while reducing experimental cost and development time [39,40,53,54].

In the longer term, intelligent thermal fluids may evolve into adaptive thermal-management platforms capable of dynamically adjusting transport characteristics in response to changing operating conditions. The integration of ZP engineering, SOTTNs, digital twins, autonomous experimentation, and AI-driven optimization could ultimately transform thermal-fluid development from empirical experimentation to self-optimizing materials design.

Figure 8 presents a conceptual roadmap for the future development of autonomous intelligent thermal fluids. The roadmap highlights the convergence of ZP-engineered nanoparticle networks, AI-driven modeling, digital-twin technologies, and autonomous experimentation into a unified materials-discovery ecosystem. By integrating real-time data acquisition, physics-informed learning, and multi-objective optimization, future thermal fluids may evolve from passive coolants into self-optimizing thermal-management platforms capable of adapting to changing operating conditions and accelerating the deployment of advanced cooling technologies.

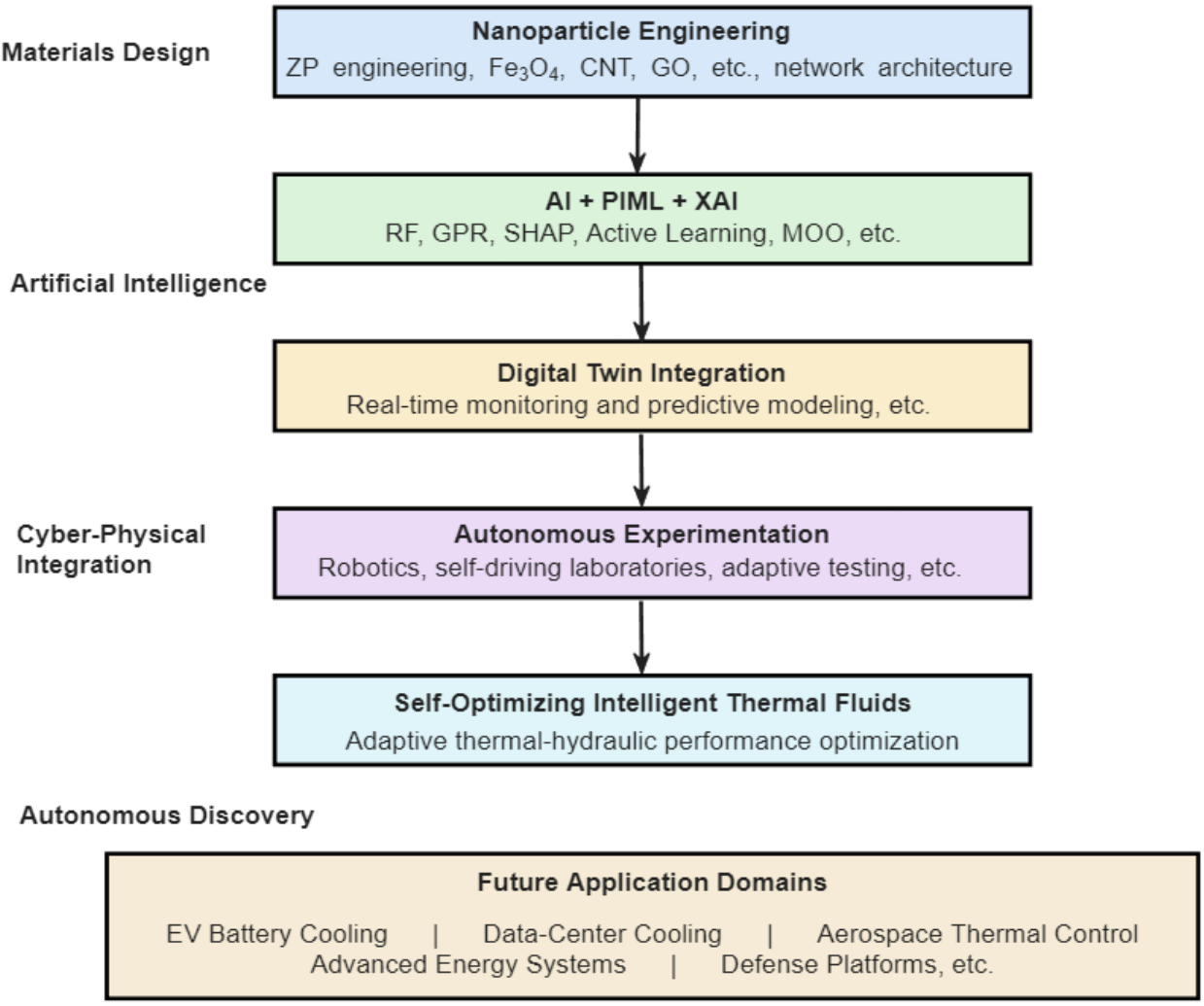


Figure 8. Future Roadmap Toward Autonomous Intelligent Thermal Fluids.

4. CASE STUDY: AI-DRIVEN DESIGN AND OPTIMIZATION OF ZP-ENGINEERED Fe_3O_4-CNT-GO NANOFLUIDS

To demonstrate the practical implementation of the AI-driven framework discussed in this work, the ZP-engineered Fe_3O_4-CNT-GO nanofluids were selected as a representative case study, involving the development of a literature-derived nanofluid database, AI-based property prediction and accuracy evaluation, feature-importance analysis, SHAP interpretation, and MOO of ZP-engineered Fe_3O_4-CNT-GO nanofluids for advanced thermal management systems, coding based on MATLAB (MATLAB version: R2024b, MathWorks, Inc. Natick, Massachusetts, USA) software, and corresponding AI models and functions were developed for conducting this case study. Figure 9 shows the schematic workflow of this case study representing AI-driven nanofluid design and optimization procedures. The workflow integrates experimental literature data, physics-informed descriptors, GPR

and RF modeling, and NSGA-II-based Pareto optimization to identify optimal nanofluid formulations that simultaneously maximize the thermal performance and stability while minimizing the dynamic viscosity and cost.

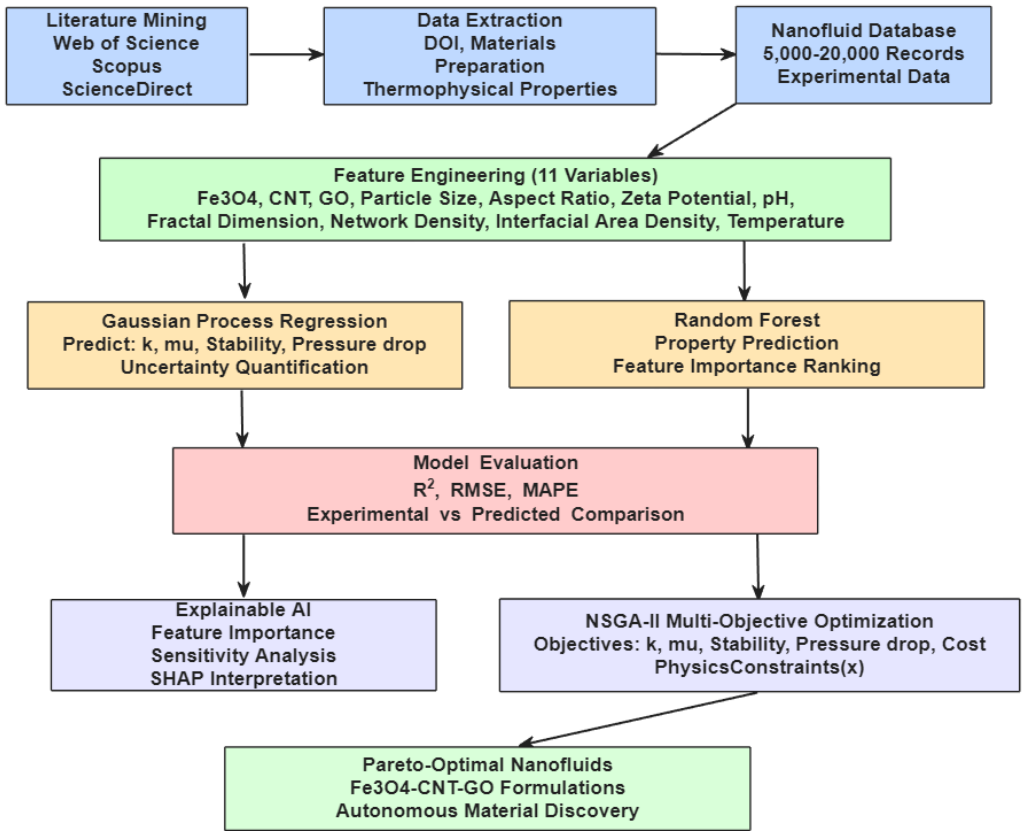


Figure 9: AI-driven design and optimization workflow of the case study for advancing nanofluids.

4.1 Literature-Derived Database Construction

For an AI-driven design and optimization platform for advancing nanofluids, the first step is the construction of a comprehensive database. The database should be designed as a materials-informatics repository rather than a simple thermophysical-property table [40,78]. The objective is to link nanoparticle descriptors to processing conditions, microstructure/network topology, thermophysical properties, and thermal management performance metrics. In this case study, the database was constructed by extracting data points from published experimental studies. Relevant publications can be collected from Web of Science, Scopus, Engineering Village, ScienceDirect, SpringerLink, ACS Publications, Wiley Online Library, and IEEE Xplore using keyworks, such as nanofluid thermal conductivity, nanofluid viscosity, hybrid nanofluids, graphene oxide nanofluids, CNT nanofluids, Fe_3O_4 nanofluids, battery cooling nanofluids, heat transfer coefficient nanofluids, etc. Each experimental condition reported in a publication is treated as an independent database record. Thus, a single article reporting multiple concentrations and temperatures may contribute tens or even hundreds of data points. Following database cleaning and validation, the resulting repository may contain 5000-20000 individual records suitable for ML applications. In

519 this study, 10000 individual records were collected. Table 3 schematically shows the sample data points collected in
520 the database.

521 **Table 3**. Sample data points collected in the database.

ID	Fluid	x_1	x_2	x_3	x_4	x_5	x_6	x_7	x_8	x_9	x_{10}	x_{11}	Y_1	Y_2	Y_3	Y_4
NF00001	Water	0.01	0.001	0.001	5	50	20	5.5	1.5	0.1	10	20	0.6391	0.8936	57.5	3.22
NF00002	Water-EG 50:50	0.011	0.004	0.008	6	51	21	5.6	1.51	0.11	11	21	0.4591	4.0622	58.41	4.02
NF00003	EG	0.012	0.007	0.015	7	52	22	5.7	1.52	0.12	12	22	0.319	16.5347	59.32	7.13
NF00004	PG	0.013	0.01	0.022	8	53	23	5.8	1.53	0.13	13	23	0.29	53.9992	60.23	16.5
NF00005	PAO	0.014	0.013	0.029	9	54	24	5.9	1.54	0.14	14	24	0.233	7.5592	61.14	4.89
NF09996	Water	0.9951	0.186	0.166	42	295	57	9	1.75	0.15	332	47	1.2536	1.4457	86.85	3.36
NF09997	Water-EG 50:50	0.9961	0.189	0.173	43	296	58	9.1	1.76	0.16	333	48	1.0735	6.5433	87.76	4.64
NF09998	EG	0.9971	0.192	0.18	44	297	59	9.2	1.77	0.17	334	49	0.9335	26.521	88.67	9.63
NF09999	PG	0.9981	0.195	0.187	45	298	60	9.3	1.78	0.18	335	50	0.9045	86.2533	89.58	24.6
NF10000	PAO	0.9991	0.198	0.194	46	299	20	9.4	1.79	0.19	336	51	0.7859	12.0252	57.69	6.01

522 Note: EG = ethylene glycol, PG = propylene glycol, and PAO = polyalphaolefin,

523

524 In this study (referring Table 3), eleven input variables (feature descriptors) were selected to characterize
525 nanofluid composition, colloidal behavior, network architecture, and operating conditions:

526 $$X = [x_1, x_2, x_3, \dots, x_{11}] \quad (1)$$

527 where $x_1 = \phi Fe_3O_4$ (loading, wt%), $x_2 = \phi CNT$ (loading, wt%), $x_3 = \phi GO$ (loading, wt%), $x_4 = d_p$ (particle size, nm),
528 x_5 = AR (aspect ratio), $x_6 = \zeta$ (ZP, mV), $x_7 = pH$, $x_8 = D_f$ (fractal dimension), x_9 = ND (network density), $x_{10} = IAD$
529 (interfacial area density), and x_{11} = T (temperature, °C), respectively. The four output variables (performance
530 metrics) describing nanofluid performance are:

531 $$Y = [Y_1, Y_2, Y_3, Y_4] \quad (2)$$

532 where $Y_1 = k$ (thermal conductivity, W/(m·K)), $Y_2 = \mu$ (dynamic viscosity, mPa·s), $Y_3 = st$ (stability index), and $Y_4 =$
533 pd (pressure drop, kPa), respectively.

534 It is worth noting that these units used for the feature descriptors (input variables) and performance metrics
535 (output variables) will be used throughout this section for the case study.

536 Additional metadata may include the DOI, publication source, measurement uncertainty, preparation route,
537 sonication time, surfactants, storage duration, convection coefficient, pumping power, performance evaluation
538 criterion, and application category, etc.

539 *4.2 AI-Based Property Prediction*

540 The GPR is particularly attractive for nanofluid datasets because it performs accurately with relatively small
541 experimental datasets and provides uncertainty estimates that can subsequently be incorporated into active learning
542 and MOO schemes [65]. The GPR establishes a probabilistic mapping between the input feature vector X and target
543 properties Y:

$$Y = [Y_1, Y_2, Y_3, Y_4] = [f_k(X), f_\mu(X), f_{st}(X), f_{pd}(X)] \quad (3)$$

using a covariance kernel $K(X_i, X_j)$, frequently chosen as the automatic relevance determination squared-exponential kernel. Separate GPR models were trained for each target property.

RF models are trained as complementary surrogate models because they are robust against experimental noise and nonlinear feature interactions. The RF framework constructs an ensemble of decision trees and predicts nanofluid properties through aggregated voting. Analogous models were developed for thermal conductivity, dynamic viscosity, stability, and pressure drop predictions. RF models are particularly valuable because they provide quantitative feature-importance rankings, allowing interpretation of the governing mechanisms underlying nanofluid performance [81].

During the model training process, the total datasets were split into training datasets and testing (validation) datasets, in this study, 80% of the total datasets for training and the rest 20% of the total datasets for testing.

Prediction accuracy is evaluated using the coefficient of the determination (R^2), root mean square error (RMSE), and mean absolute percentage error (MAPE):

$$R^2 = 1 - \frac{\sum(y_i - \hat{y}_i)^2}{\sum(y_i - \bar{y})^2} \quad (4)$$

$$RMSE = \sqrt{\frac{1}{N}\sum(y_i - \hat{y}_i)^2} \quad (5)$$

$$MAPE = \frac{1}{N}\frac{\sum(y_i - \hat{y}_i)}{\sum y_i} \times 100(\%) \quad (6)$$

where y_i, $\hat{y}_i$, and $\bar{y}$ denote experimental, predicted, and mean values, respectively.

As shown in Table 4, the predictive performance of the GPR and RF models varies considerably across the four target properties. For the thermal conductivity (k), the RF model exhibited substantially better predictive capability, achieving an R^2 value of 0.9967 compared with only 0.3170 for the GPR model, while reducing the RMSE from 0.1629 to 0.0113 and the MAPE from 20.22% to 1.29%. For the pressure drop, the RF model exhibited substantially better predictive capability, achieving an R^2 value of 0.9986 compared with only 0.0042 for the GPR model, while reducing the RMSE from 6.3875 to 0.2359 and the MAPE from 72.67% to 1.81%. Although the GPR models achieved nearly perfect predictions for the dynamic viscosity and stability index ($R^2 \approx 1.0000$), the RF models also maintained excellent accuracy with R^2 values between 0.9986 and 0.9991.

Table 4. Comparison of error metrics based on GPR and RF models.

Error Metrics	Thermal Conductivity (k)		Dynamic Viscosity (μ)		Stability Index		Pressure Drop	
	GPR	RF	GPR	RF	GPR	RF	GPR	RF
R^2	0.3170	0.9967	1.0000	0.9986	1.0000	0.9991	0.0042	0.9986
RMSE	0.1629	0.0113	0.0112	0.9478	0.0001	0.3186	6.3875	0.2359
MAPE	20.2246	1.2948	0.1691	8.9652	0.0001	0.3105	72.6664	1.8063

Overall, the RF models demonstrated consistently high predictive accuracy and robust generalization capabilities across all performance metrics. In contrast, the GPR models exhibited limitations in predicting thermal conductivity and pressure drop, as it fails to capture the nonlinear relationships among nanofluid parameters. In

practice, the magnitude of the prediction error depends on the specific model constructed using training and validation datasets for each modeling run. The superior performance of the RF models can be attributed to their ability to effectively capture the highly nonlinear interactions among nanoparticle composition, ZP, network density, fractal dimension, and other physicochemical descriptors. Consequently, the RF models were selected as the preferred surrogate models for subsequent feature-importance analysis and multi-objective optimization because of their greater robustness and overall predictive reliability.

For better understanding the prediction accuracy by GPR and RF models, according to the above error metrics data listed in Table 4, Figure 10 compares the pressure drop predictions obtained from the GPR and RF models against the corresponding experimental values. The RF predictions (red symbols) closely follow the 45° reference line over the entire range of pressure drops, indicating excellent agreement between predicted and experimental values and demonstrating the strong predictive capability of the RF model. In contrast, the GPR predictions (blue symbols) exhibit significant deviations from the 45° line, particularly at higher pressure drops, where substantial underprediction and increased data dispersion are observed. The presence of several clustered and nonlinear prediction bands further suggests that the GPR model was unable to fully capture the complex relationships among the nanofluid composition, network topology, and thermochemical performance. These observations are consistent with the quantitative results reported in Table 4. Overall, Figure 10 clearly demonstrates that the RF model provides superior accuracy, robustness, and generalization performance for predicting thermochemical performance (target properties) in the present nanofluid dataset, making it a more suitable surrogate model for subsequent feature-importance analysis and NSGA-II-based multi-objective optimization.

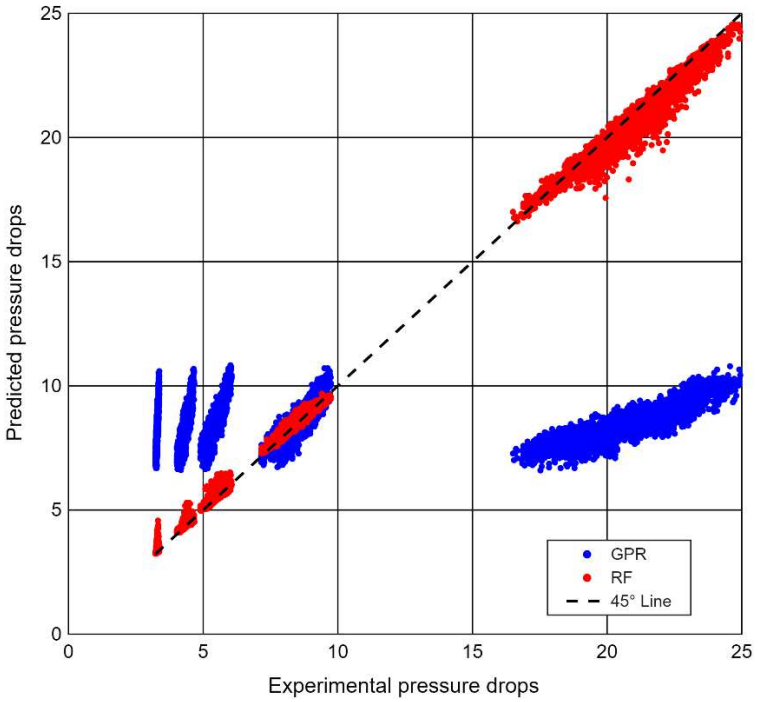


Figure 10: Comparison of pressure drops of experimental and predicted values by GPR and RF models.

595

596 *4.3 Parameter Importance and Explainable AI Analysis*

597 A major objective of the AI-driven advanced nanofluid discovery is to identify which physicochemical
598 descriptors most strongly influence thermophysical performance. For RF models, predictor importance can be
599 calculated by using the MATLAB function predictorImportance(). In METLAB, the function predictorImportance()
600 is designed for the feature importance analysis of tree-based and ensemble models [81]. It calculates parameter
601 importance by summing the total reduction in node risk (impurity or error) caused by splits on a specific predictor
602 and then dividing that sum by the total number of branch nodes. It evaluates how effectively a feature organizes data
603 across all decision trees within the RF ensemble. Using the eleven-feature variable *X*, the relative importance of each
604 variable (feature) can be calculated directly from the trained RF model.

605 The MATLAB function predictorImportance() works for an RF model. Unlike RF models, the GPR does not
606 directly support the MATLAB function predictorImportance(). However, there are alternative approaches for feature
607 importance analysis based on GPR models. The most rigorous GPR-based feature importance analysis method is the
608 automatic relevance determination (ARD). When an ARD kernel is employed, the feature relevance can be
609 quantitatively determined from the optimized kernel length scales learned during model training. For the ARD
610 squared-exponential kernel:

611 $$k(xi, xj) = \sigma_f^2 \exp\left\{-\frac{1}{2}\sum_{m=1}^{M}\frac{(x_{im}-x_{jm})^2}{l_m^2}\right\} \quad (7)$$

612 where l_m = characteristic length scale of feature m

613 σ_f = signal variance

614 M = 11 input features

615 The ARD automatically assigns an independent length scale to each input feature [65]. Features with smaller
616 characteristic length scales have greater influence on the target variable because they response to changes rapidly
617 with those inputs.

618 To facilitate interpretation, a normalized relevance score is defined as:

619 $$RI_m = \frac{1/l_m}{\sum_{j=1}^{M}(1/l_j)} \quad (8)$$

620 where RI_m is the relative importance of feature m.

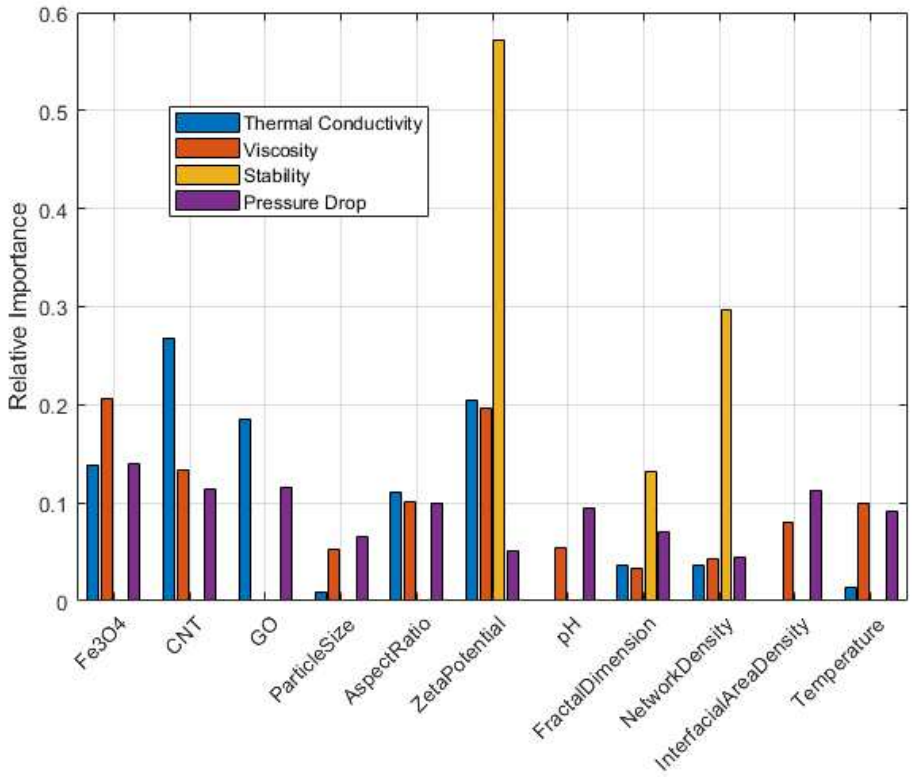
621 As summarized in Table 5, both the GPR and RF models consistently identify nanoparticle composition and
622 network-related descriptors as the dominant factors governing nanofluid performance, although the relative rankings
623 slightly differ between the two approaches. For the thermal conductivity, the CNT concentration (x_2), GO
624 concentration (x_3), ZP (x_6), and pH (x_7) were identified by the GPR model as the most influential variables,
625 highlighting the importance of conductive carbon nanostructures and electrostatically controlled network formation.
626 The RF model exhibited a similar trend, with CNT, GO, and Fe_3O_4 concentrations ranking among the most
627 important factors. For the dynamic viscosity, the CNT concentration was the overwhelmingly dominating factor by
628 the GPR predictions, whereas the RF model indicated that the network density, CNT concentration, and GO

concentration jointly contributed to viscosity behavior. Regarding stability, the ZP and network density emerged as the most critical descriptors by both GPR and RF models, confirming the fundamental role of electrostatic stabilization and network architecture in maintaining colloidal stability. For the pressure drop, both GPR and RF models showed that CNT, ZP, and Fe_3O_4 and GO concentrations were the primary controlling variables reflecting the strong influence of the nanoparticle loading on flow resistance. Overall, the results demonstrate that the nanoparticle composition, ZP, network density, and fractal characteristics are the key design parameters controlling thermophysical performance, providing strong support for the concept of SOTTNs and their use as optimization variables in AI-driven nanofluid design.

Table 5: Summary of the parameter (input feature) importance on the four nanofluid thermophysical properties (output target properties) based on GPR and RF models.

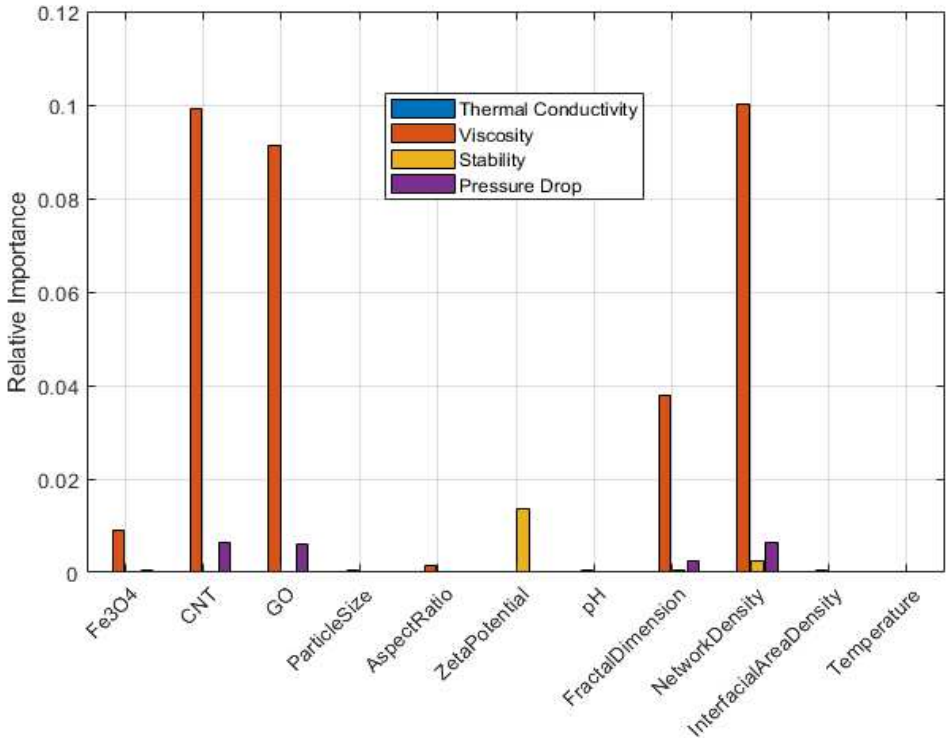
Input feature (descriptor)	Thermal conductivity		Dynamic viscosity		Stability Index		Pressure Drop	
	GPR	RF	GPR	RF	GPR	RF	GPR	RF
x_1 (Fe_3O_4)	0.1375	0.0573×10^{-5}	2.587×10^{-7}	0.00836	1.136×10^{-6}	2.704×10^{-5}	0.1452	0.00053
x_2 (CNT)	0.2675	0.2415×10^{-5}	0.9999	0.09514	1.208×10^{-6}	1.540×10^{-5}	0.1161	0.00596
x_3 (GO)	0.1846	0.1491×10^{-5}	0.0001	0.08776	1.240×10^{-6}	1.398×10^{-5}	0.1142	0.00540
x_4 (ParticleSize)	0.0083	0.0005×10^{-5}	6.313×10^{-12}	0.00053	1.222×10^{-6}	1.696×10^{-5}	0.0548	3.283×10^{-5}
x_5 (AspectRatio)	0.1104	0.0032×10^{-5}	6.160×10^{-12}	0.00162	1.183×10^{-6}	0.00011	0.1005	1.006×10^{-4}
x_6 (ZetaPotential)	0.2048	0.0041×10^{-5}	3.439×10^{-12}	0.00027	0.5720	0.01391	0.0508	1.673×10^{-5}
x_7 (pH)	0.0001	0.0024×10^{-5}	1.666×10^{-11}	0.00063	1.211×10^{-6}	2.016×10^{-5}	0.0874	4.048×10^{-5}
x_8 (FractalDimension)	0.0362	0.0066×10^{-5}	6.748×10^{-8}	0.03880	0.1314	0.00039	0.0650	0.00242
x_9 (NetworkDensity)	0.0364	0.0149×10^{-5}	2.232×10^{-12}	0.10346	0.2966	0.00235	0.0460	0.00638
x_{10} (InterfacialAreaDensity)	0.0001	0.0006×10^{-5}	9.633×10^{-12}	0.00054	1.257×10^{-6}	2.591×10^{-5}	0.1082	3.438×10^{-5}
x_{11} (Temperature)	0.0141	0.0005×10^{-5}	2.740×10^{-12}	0.00029	1.141×10^{-6}	2.125×10^{-5}	0.0882	1.710×10^{-5}

Figure 11 provides a visual comparison summary of the feature importance obtained from the GPR-ARD and RF models for the four target properties. Although the two modeling approaches assign different numerical weights to individual descriptors, both reveal that nanofluid performance is governed primarily by a relatively small set of key variables rather than by all eleven inputs equally. The GPR-ARD results (Figure 11(a)) exhibit a more physically interpretable distribution, highlighting the strong contributions of the nanoparticle loading (Fe_3O_4 loading, CNT loading, and GO loading), ZP, network density, fractal dimension, and aspect ratio, thereby emphasizing the importance of conductive network formation and electrostatic interactions in controlling thermal transport and stability. In contrast, the RF results (Figure 11 (b)) show a more concentrated importance distribution, with a few dominant variables accounting for most of the predictive power, particularly CNT and GO concentrations for the viscosity-related behavior and the network density and ZP for stability. Overall, the agreement between the two independent ML approaches indicates that nanoparticle composition and ZP and network-topology descriptors consistently exert the greatest influence on thermophysical performance, whereas the particle size, interfacial area density, pH, and temperature play comparatively minor roles within the studied design space. These findings further support the concept that optimizing SOTTNs is more effective than simply increasing nanoparticle loading for achieving enhanced nanofluid performance.



657

658 (a) GPR-ARD models



659

660 (b) RF models

Figure 11: comparison of parameter (input feature) importance on four nanofluid thermophysical properties (target properties) based on (a) GPR and (b) RF models.

To further enhance interpretability, SHAP analysis provides a more interpretable analysis than RF importance ranking or GPR-ARD alone because it quantifies both global importance, indicating most important variables overall, and local importance, explaining a specific nanofluid formulation with a particular prediction [46,70,79]. SHAP values are grounded in the cooperative game theory and distributes prediction contributions among all predictor variables. The SHAP value of feature *i* is:

$$\emptyset_i = \sum_{S \subseteq F \setminus \{i\}} \frac{|S|!(M-|S|-1)!}{M!} [f(S \cup \{i\}) - f(S)] \quad (9)$$

where M = total number of features

S = subset of available features

$f(\cdot)$ = trained machine-learning model

The total prediction can be decomposed as:

$$\hat{y} = \emptyset_0 + \sum_{i=1}^{M} \emptyset_i \quad (10)$$

where ϕ_0 represents the average prediction of the training dataset. Such analyses provide direct physical insights into the relationship between electrostatic interactions, percolation behavior, and macroscopic thermophysical properties [70].

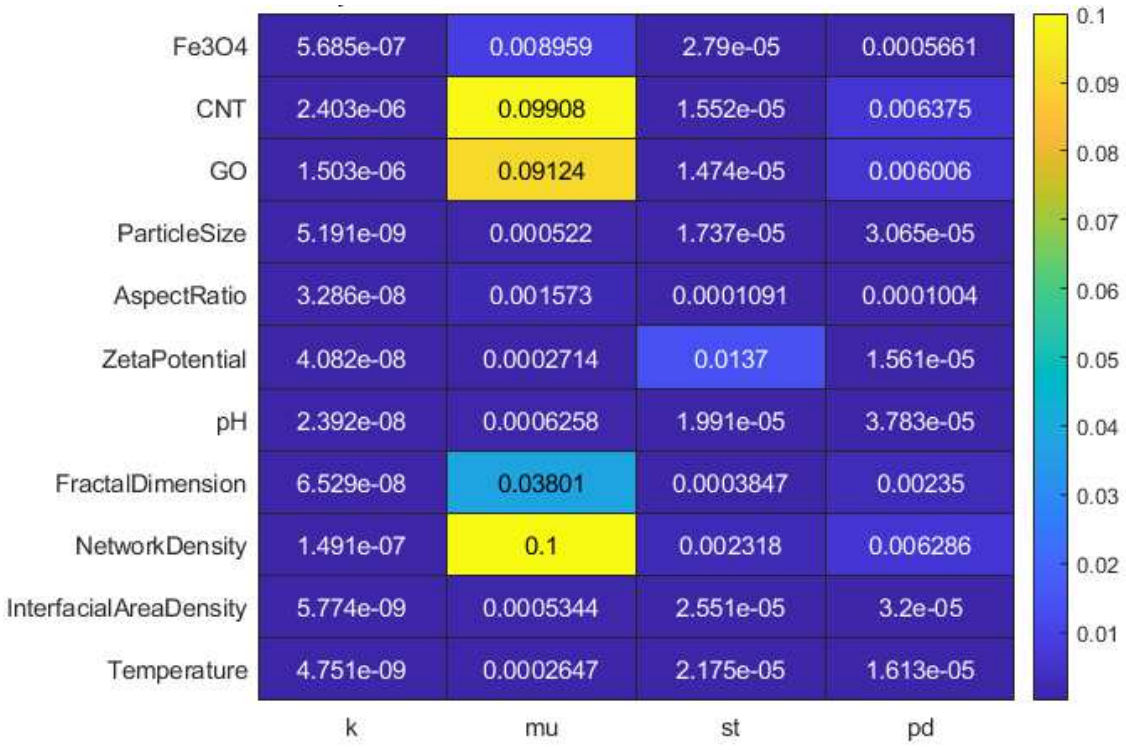
As shown in Table 6, the SHAP analysis provides local interpretability of the RF and GPR models by quantifying both the magnitude and direction of each predictor's contribution to individual predictions. The results indicate that the CNT concentration, GO concentration, and ZP exert the strongest local effects on thermal conductivity, while CNT and GO concentrations are the primary contributors to dynamic viscosity and pressure drop predictions. For the stability index, ZP and pH consistently exhibit the largest positive SHAP values, emphasizing the critical role of electrostatic stabilization in maintaining suspension stability. Although the RF and GPR models assign different contribution magnitudes to specific variables, both approaches consistently identify the nanoparticle composition, ZP, and network-related descriptors as the dominant factors governing nanofluid performance. These findings provide a physically meaningful explanation of the machine-learning predictions and reinforce the importance of controlling nanoparticle interactions and thermal-network formation in the design of high-performance nanofluids.

Table 6: Summary of the parameters (predictors)' local Shapley Values for the four nanofluid thermophysical properties (output target properties) based on the RF and GPR models.

Predictor	Thermal Conductivity		Dynamic Viscosity		Stability Index		Pressure Drop	
	RF	GPR	RF	GPR	RF	GPR	RF	GPR
x_1 (Fe_3O_4)	0.01441	0.03576	0.40426	0.36253	0.00233	-1.323×10^{-10}	0.34521	0.05769
x_2 (CNT)	-0.03281	-0.02911	-0.71147	-0.33958	-0.01649	-1.323×10^{-10}	-0.09850	-0.10674
x_3 (GO)	-0.13217	-0.09717	-3.93440	0.42222	-0.01389	-1.448×10^{-10}	-0.92147	-0.74934
x_4 (NetworkDensity)	5.322×10^{-5}	-0.00056	-0.03994	0.00930	0.00267	-1.456×10^{-10}	0.00793	-8.046×10^{-5}
x_5 (FractalDimension)	-0.00844	-0.01030	-0.01551	0.01036	-0.01464	-1.070×10^{-10}	0.00106	-2.750×10^{-5}

x_6 (ZetaPotential)	0.01083	0.01530	-0.04079	0.01139	9.99620	7.92000	-0.00030	0.02997
x_7 (AspectRatio)	-2.456×10^{-5}	0.00032	-0.02586	0.01170	-0.00075	-1.148×10^{-10}	-0.02876	-8.268×10^{-5}
x_8 (pH)	0.00043	0.00747	-0.45737	-0.12423	1.92220	2.02030	0.01896	-0.00013
x_9 (InterfacialAreaDensity)	-0.01245	-1.509×10^{-5}	0.03928	0.01198	-4.93460	-5.71650	0.48928	-0.19671
x_{10} (ParticleSize)	-9.363×10^{-5}	2.492×10^{-6}	-0.03939	0.012293	-0.00642	-1.127×10^{-10}	-0.00517	-0.01997
x_{11} (Temperature)	-0.00020	2.577×10^{-6}	0.043994	0.012293	0.01015	-9.907×10^{-11}	0.00537	-0.01002

Figure 12 compares the global SHAP importance distributions obtained from the RF and GPR models for the thermal conductivity (k), dynamic viscosity (μ), stability index (st), and pressure drop (pd). Although the two models assign different quantitative importance values, both consistently identify nanoparticle composition and network-related descriptors as the primary drivers of nanofluid performance. The RF model emphasizes the CNT concentration, GO concentration, and network density as the dominant factors affecting the dynamic viscosity and pressure drop, whereas the GPR model highlights the nanoparticle concentrations and zeta potential for thermal conductivity and the ZP and network density for stability. The stronger sensitivity of the GPR model to ZP and stability-related descriptors suggests its greater ability to capture electrostatic and network-interaction effects, while the RF model focuses more on composition-dependent nonlinear relationships. Overall, both heatmaps indicate that the nanoparticle loading, ZP, and network topology play central roles in determining nanofluid thermophysical behavior, supporting their selection as key design variables for AI-driven optimization.



(a)



(b)

Figure 12: Heatmap representation for global SHAP importance for four performance indicators based on (a) RF and (b) GPR models.

4.4 Surrogate-Based MOO- NSGA-II Pareto Optimization

The trained surrogate models are subsequently embedded within a MOO framework. The design objective is to simultaneously:

Maximize: $f_1 = k,$ and $f_3 = st$ and minimize $f_2 = \mu, f_4 = pd, and\ f_5 = Cost.$ (11)

where the cost function is approximated by:

$$Cost = 20 \cdot \phi Fe3O4 + 250 \cdot \phi CNT + 180 \cdot \phi GO \quad (12)$$

Reflecting the higher material cost of CNTs and graphene-based oxide nanostructures.

The objective function used by the Non-dominated Sorting Generic Algorithm II (NSGA-II) for MOO is implemented in MATLAB [74].

Unlike purely data-driven optimization, physically realistic design constraints (physics-informed constraints) are imposed to ensure feasible formulations.

Percolation Constraint: The total nanoparticle loading must exceed the percolation threshold:

$$\emptyset_{total} = \emptyset_{Fe3O4} + \emptyset_{CNT} + \emptyset_{GO} > \emptyset_c \quad (13)$$

where $\emptyset_c = \frac{0.6}{AR}$ ensures formation of a continuous thermal transport network.

Colloidal Stability Constraint: Stable suspensions require:

$$|\varsigma| \geq 30mV \quad (14)$$

to suppress aggregation and sedimentation.

Network Connectivity Constraint: A Thermal Network Connectivity Index (TNCI) is introduced:

$$TNCI = \frac{ND \cdot AR}{100 D_f} \text{ and constrained as: TNCI} \geq 1 \quad (15)$$

to ensure sufficient conductive network connectivity.

The optimization is carried out by using MATLAB's NSGA-II implementation (gamultiobj() function) [82]. At each generation, NSGA-II generates candidate nanofluid formulation, evaluates performance using the trained GPR surrogate models, applies physical constraints, conducts non-dominated sorting, identifies Pareto-optimal solutions, and evolves future generations through crossover and mutation [74,82].

Table 7 summarizes the convergence behavior of the NSGA-II (gamultiobj) optimization based on the RF surrogate models. During the early generations, the average Pareto distance and spread exhibited relatively large fluctuations as the algorithm explored the design space and identified feasible trade-off solutions. As the optimization progressed, the average Pareto distance gradually decreased from approximately 10^{-1} to 7.7×10^{-3}, indicating a high degree of convergence toward the Pareto-optimal front. Meanwhile, the Pareto spread stabilized within a narrow range of 0.45-0.47, suggesting that solution diversity was maintained while convergence was achieved. The optimization terminated automatically at generation 102 because the change in Pareto spread fell below the specified function-tolerance criterion, indicating that further iterations were unlikely to yield significant improvements. These results demonstrate the effectiveness and stability of the RF-assisted NSGA-II framework in identifying optimal nanofluid formulations while maintaining a well-distributed Pareto front.

Table 7. Sample optimization process output data points at the beginning and the end of the iterations based on the RF models.

Generation #	Function-Count	Average Pareto Distance	Average Pareto Spread
1	301	1.000000	1.000000
2	601	0.141530	0.982390
3	901	0.145909	0.323314
4	1201	0.074992	0.129378
5	1501	0.068643	0.164230
98	29401	0.007898	0.468951
99	29701	0.007754	0.453410
100	30001	0.007706	0.465986
101	30301	0.007716	0.456005
102	30601	0.007755	0.458479

The resulting Pareto front provides a set of optimal trade-off solutions balancing the thermal conductivity, dynamic viscosity, stability, heat-transfer enhancement, and economic considerations [71,72,74].

Figure 13 illustrates the Pareto front obtained from the RF-assisted MOO (three-objective optimization enabling 3D plot displaying), demonstrating the trade-offs among the three selected objectives. The distribution of Pareto-optimal solutions indicates that no single nanofluid formulation simultaneously optimizes all objectives, highlighting

the inherent conflicts among thermal performance, flow behavior, and stability-related characteristics. The relatively well-distributed Pareto front suggests that the NSGA-II algorithm successfully identified a diverse set of non-dominated solutions spanning the feasible design space. Consequently, the Pareto-optimal formulations provide decision-makers with multiple candidate nanofluids that balance competing performance requirements, enabling selection based on specific thermal management objectives and operational constraints.

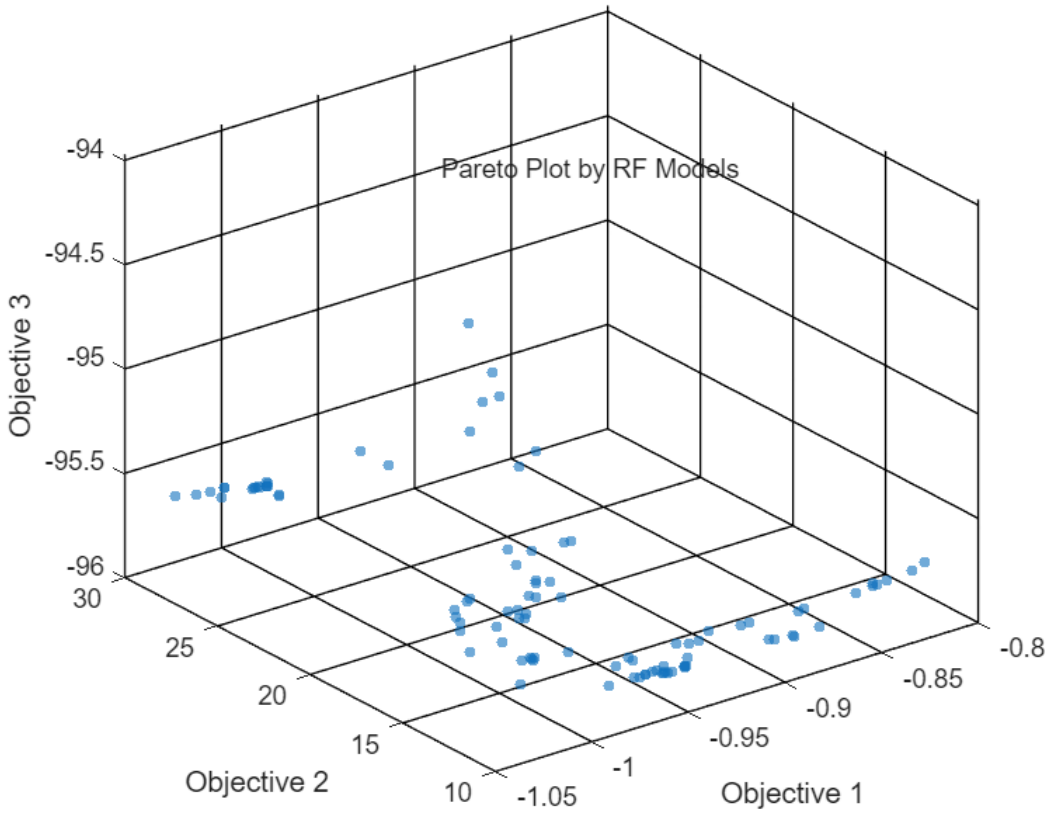


Figure 13: Pareto front plot showing three objectives MOO based on RF models.

Table 8 presents the Pareto-optimal solutions obtained from the RF-assisted NSGA-II optimization, demonstrating the trade-offs among the thermal conductivity (f_1), dynamic viscosity (f_2), stability index (f_3), pressure drop (f_4), and cost (f_5). The optimized solutions span thermal conductivity values of approximately 0.89-1.04 W/(m·K), stability indices above 94.5, and costs ranging from 23.0 to 29.8, illustrating the inherent conflicts among performance objectives. In general, solutions with higher thermal conductivities tend to be associated with increased dynamic viscosities, pressure drops, and costs, whereas lower-cost formulations often exhibit slightly reduced thermal performance. Despite these trade-offs, all Pareto-optimal solutions maintain high stability indices, indicating that the imposed physics-informed constraints effectively preserved colloidal stability while optimizing thermal-hydraulic performance. The results demonstrate that the RF-assisted NSGA-II framework successfully identifies a diverse set of feasible nanofluid formulations that balance the conductivity enhancement, hydraulic

efficiency, stability, and economic considerations, providing valuable design options for application-specific thermal management systems.

Table 8. The output results of the Pareto optimized design objectives based on RF models.

Generation #	f_1 (thermal conductivity)	f_2 (viscosity)	f_3 (stability index)	f_4 (pressure drop)	f_5 (cost)
1	1.0000	11.1612	95.0897	5.7974	6.4605
2	1.0445	12.7562	95.3725	6.0796	22.7602
3	0.9506	10.1324	95.7853	5.6275	36.7094
4	0.9178	10.0936	95.6700	5.6073	21.5188
5	0.9906	28.5598	95.6663	9.7313	4.4647
98	1.0096	28.8120	95.6304	9.8433	8.9555
99	0.9730	10.2652	95.7813	5.6319	25.0187
100	1.0431	12.0781	94.4847	6.0149	22.9767
101	0.8889	10.1281	95.6843	5.6276	29.8283
102	0.9887	10.2652	95.7746	5.6319	24.2548

Table 9 summarizes the Pareto-optimal combinations of the eleven design variables identified by the RF-assisted NSGA-II optimization. The optimized solutions exhibit relatively narrow ranges of the CNT concentration, zeta potential, aspect ratio, network density, interfacial area density, and temperature, suggesting that these parameters are strongly constrained by the simultaneous requirements of the high thermal conductivity, low dynamic viscosity and pressure drop, and high stability. In contrast, Fe_3O_4 and GO concentrations show greater variability among the Pareto solutions, indicating additional design flexibilities for balancing performance and cost. Notably, all Pareto-optimal solutions correspond to high zeta potentials (approximately 48–56 mV), large aspect ratios (approximately 300–470), and high network densities (approximately 0.78–1.00), confirming the importance of electrostatic stabilization and well-connected thermal transport networks. Overall, the optimization results demonstrate that superior nanofluid performance is achieved through a coordinated combination of nanoparticle composition, network topology, and colloidal characteristics rather than through maximizing any single design variable.

Table 9. The output results of the Pareto optimized input features based on RF models.

Generation #	x_1 (Fe_3O_4)	x_2 (CNT)	x_3 (GO)	x_4 (d_p)	x_5 (AR)	x_6 (ZP)	x_7 (pH)	x_8 (D_f)	x_9 (ND)	x_{10} (IAD)	x_{11} (T)
1	0.1284	0.0094	0.0086	28.606	451.13	49.072	8.1488	2.1336	0.8060	292.94	70.068
2	0.9919	0.0100	0.0024	36.912	298.78	55.799	9.2169	1.6973	0.8557	269.98	74.263
3	0.9211	0.0097	0.0881	32.636	451.64	50.608	8.1858	2.0771	0.9891	282.48	73.652
4	0.1244	0.0096	0.0924	29.807	361.58	50.427	8.0235	1.8987	0.9911	274.20	72.453
5	0.1220	0.0017	0.0090	29.013	468.21	48.741	7.9698	2.1438	0.9759	291.88	70.198
98	0.3097	0.0053	0.0080	30.324	432.67	50.813	8.3949	2.0986	0.9757	296.21	72.921
99	0.9300	0.0099	0.0219	34.969	402.18	52.154	7.9761	1.8214	0.9944	269.84	73.544
100	0.9911	0.0099	0.0037	36.591	323.34	54.293	9.0265	1.6873	0.7816	271.68	73.750
101	0.8060	0.0139	0.0568	27.650	466.30	48.013	8.3859	2.0955	0.9952	290.68	73.245
102	0.9498	0.0077	0.0185	34.122	395.62	52.348	7.9396	1.7734	0.9922	273.54	73.535

789

790 *4.5 Implications for Autonomous Materials discovery*

791 Overall, the case study presented collectively demonstrates a paradigm shift from conventional trial-and-error
792 materials research toward closed-loop, autonomous discovery ecosystems. The proposed workflow demonstrates
793 how literature-derived experimental data, across diverse materials domains, the integration of foundation models,
794 PIML, XAI, MOO can be integrated into a unified AI-driven material discovery platform [40,43,78], enabling
795 accelerated navigation of vast compositional and process spaces while substantially reducing experimental burden.
796 Beyond improvements in predictive accuracy, these studies highlight the emergence of adaptive systems capable of
797 generating hypotheses, quantifying uncertainty, and iteratively optimizing experiments with minimal human
798 intervention. Importantly, the convergence of data-centric AI with automated synthesis and characterization
799 establishes a scalable framework for continuously expanding materials knowledge. These advances, coupling with
800 active learning, digital twins, robotic experimentation, and real-time sensing, could ultimately enable autonomous
801 discovery of materials intelligent thermal fluids tailed for EV battery cooling, data-center thermal management,
802 aerospace thermal control, and next-generation adaptive cooling systems [43,46,47,79,80].

803

804 ## 5. CONCLUSIONS AND FUTURE PERSPECTIVES

805 Nanofluids have emerged as promising thermal fluids for next-generation thermal management systems.
806 However, this research work demonstrates that the thermal conductivity enhancement alone is insufficient for
807 practical implementation. Successful deployment requires the simultaneous optimization of thermal conductivity,
808 dynamic viscosity, dispersion stability, corrosion resistance, manufacturability, economic viability, and long-term
809 reliability. The strong coupling among nanoparticle composition, morphology, surface chemistry, ZP, interfacial
810 interactions, rheological behavior, and thermal transport mechanisms makes nanofluid design a highly nonlinear and
811 multi-objective problem that is difficult to address using conventional empirical approaches.

812 Recent advances in AI/ML, PIML, and MOO are transforming nanofluid development from trial-and-error
813 experimentation toward predictive and data-driven materials design. Particular attention has been given to ZP-
814 engineered nanofluids, in which electrostatic interactions are deliberately controlled to promote multidimensional
815 SOTTNs. By integrating positively charged Fe_3O_4 nanoparticles, high-aspect-ratio CNTs, and GO nanosheets, these
816 architectures can simultaneously enhance thermal transport, improve colloidal stability, and reduce the traditional
817 conductivity-viscosity trade-off that has historically limited commercial adoption.

818 The case study presented in this work further demonstrates the practical implementation of an AI-driven
819 nanofluid design framework. A literature-derived nanofluid database was constructed using eleven physicochemical
820 descriptors as input features and four key thermophysical properties as target variables. GPR and RF models were
821 trained for property prediction, feature-importance analysis, and explainable-AI interpretation. The results showed
822 that the nanoparticle composition, ZP, network density, and fractal characteristics are among the most influential
823 descriptors governing the thermal conductivity, dynamic viscosity, stability, and pressure-drop behavior. RF models

exhibited superior predictive performance and served as reliable surrogate models for subsequent optimization. Integration of SHAP analysis further provided physically interpretable insights into the relationships among the nanoparticle interaction, network topology, and macroscopic performance.

Looking forward, future research should focus on the development of large standardized nanofluid databases, explainable and physics-informed AI frameworks, autonomous experimentation platforms, digital twins, and self-driving laboratories. Additional emphasis should be placed on long-term stability, corrosion behavior, lifecycle assessment, manufacturing scalability, and techno-economic optimization. The convergence of ZP engineering, SOTTNs, ML, autonomous experimentation, and digital manufacturing is expected to enable the emergence of intelligent thermal fluids capable of adaptive performance and rapid formulation optimization. Such developments may ultimately accelerate the commercialization of advanced nanofluids for EVs, data centers, advanced energy technologies, high-performance electronics, aerospace systems, and defense applications, establishing a new paradigm for AI-driven thermal management technologies.

Funding Statement: This research received no external funding.

Author Contributions: Conceptualization, Z.H. and H.H.; methodology, Z.H. and H.H.; software, Z.H.; formal analysis, Z.H.; investigation, Z.H.; resources, Z.H. and H.H.; data curation, Z.H.; writing—original draft preparation, Z.H.; writing—review and editing, Z.H. and H.H.; visualization, Z.H.; project administration, Z.H. All authors have read and agreed to the published version of the manuscript.

Competing Interests Policy: The author declares no conflicts of interest. The funders had no role in the design of the study; in the collection, analyses, or interpretation of data; in the writing of the manuscript; or in the decision to publish the results.

Dual Publication Statement: The author confirms that neither the manuscript nor any parts of its content are currently under consideration or published in another journal.

Authorship Statement: The author agrees with the content. All gave explicit consent to submit, and the author obtained consent from the responsible authorities at the institute or organization (i.e., South Dakota State University) where the work was carried out, before the work was submitted.

Data Availability Statement: Not applicable.

Acknowledgments: The authors gratefully acknowledge the support from the Department of Mechanical Engineering of J.J. Lohr College of Engineering at South Dakota State University.

Abbreviations

The following abbreviations are used in this manuscript:

AI	Artificial Intelligence
ANNs	Artificial Neural Networks
CNNs	Convolutional Neural Networks
CNTs	Carbon Nanotubes
DNNs	Deep Neural Networks
EVs	Electric Vehicles
GO	Graphene Oxide

GPR	Gaussian Process Regression
MAPE	Mean Absolute Percentage Error
ML	Machine Learning
MOO	Multi-Objective Optimization
MWCNTs	Multi-Walled Carbon Nanotubes
NSGA-II	Non-dominated Sorting Generic Algorithm II
PIML	Physics-Informed Machine Learning
R^2	Coefficient of Determination
RF	Random Forest
RMSE	Root Mean Square Error
SHAP	Shapley Additive Explanations
SOTTNs	Self-Organized Thermal Transport Networks
SVMs	Support Vector Machines
SWCNTs	Single-Walled Carbon Nanotubes
XAI	Explainable Artificial Intelligence
ZP	Zeta-Potential

REFERENCES

[1]. S.U.S. Choi, *Enhancing thermal conductivity of fluids with nanoparticles*. IMECE1995-0926, pp. 99-105, ASME International Mechanical engineering Congress and Exposition, November 12-17, 1995, San Francisco, CA, USA.

[2]. J.A. Eastman, S.U.S. Choi, S. Li, W. Yu, L.J. Thompson, Enhanced thermal conductivity through the development of nanofluids. MRS Online Proceedings Library, 457 (1996) 3-11.

[3]. H. Younes, M. Mao, S.M.S. Murshed, D. Lou, H. Hong, GP Peterson, Nanofluids: Key parameters to enhance thermal conductivity and its applications, Applied Thermal Engineering, 207 (2022) 118202

[4]. W. Yu, H. Xie, A review on nanofluids: Preparation, stability mechanisms, and applications. *Journal of Nanomaterials*, 2012, 435873.

[5]. O. Mahian, L. Kolsi, M. Amani, P. Estellé, G. Ahmadi, C. Kleinstreuer, J.S. Marshall, R.A. Taylor, E. Abu-Nada, S. Rashidi, H. Niazmand, S. Wongwises, T. Hayat, A. Kasaeian, I. Pop, Recent advances in modeling and simulation of nanofluid flows. *Physics Reports*, 790 (2019) 1-48.

[6]. E.C. Okonkwo, I. Wole-Osho, I.W. Almanassra, Y.M. Abdullatif, T. Al-Ansari, An updated review of nanofluids in various heat transfer devices, *Journal of Thermal Analysis and Calorimetry*, 145 (**2021**) 2817-2872.

[7]. S.K. Das, S.U.S. Choi, W. Yu, T. Pradeep, T. *Nanofluids: Science and Technology*. 2007, Wiley.

[8]. N.A.C. Sidik, I.M. Adamu, M.M Jamil, G.H.R. Kefayati, R. Mamat, G. Najafi, Recent progress on hybrid nanofluids in heat transfer applications: a comprehensive review. *International Communications in Heat and Mass Transfer*, 78 (2016) 68-79.

[9]. M. Alktranee, P. Bencs, Factors affecting nanofluids behaviour: a review, International Review of Applied Sciences and Engineering, 14(2) (2023) 241-255.

[10]. M.A. Rahman, S.M.M. Hasnain, S. Pandey, A. Tapalova, N. Akylbekov, R. Zairov, Review on nanofluids: preparation, properties, stability, and thermal performance augmentation in heat transfer applications, ACS Omega, 9(30 (2024), 32328-32349.

[11]. S.U.S. Choi, Z. G. Zhang, W. Yu, F.E. Lockwood, E.A. Grulke, *Anomalous thermal conductivity enhancement in nanotube suspensions.* Applied Physics Letters, 79 (2001) 2252-2254.

[12]. H. Xie, H. Lee, W. Youn, M Choi, *Nanofluids containing multiwalled carbon nanotubes and their enhanced thermal conductivities.* Journal of Applied Physics, 94 (2003) 4967-4971.

[13]. A.A. Balandin, S. Ghosh, W. Bao, I. Calizo, D. Teweldebrhan, F. Miao, C.N. Lau, *Superior thermal conductivity of single-layer graphene.* Nano Letters, 8(3) (2008) 902-907.

[14]. S. Berber, Y.K. Kwon, D. Tománek, *Unusually high thermal conductivity of carbon nanotubes.* Physical Review Letters, 84 (2000) 4613-4616.

[15]. F. Du, J.E. Fischer, K.I. Winey, *Effect of nanotube alignment on percolation conductivity in carbon nanotube/polymer composites.* Physical Review B, 72 (2005) 121404(R).
[16]. L.S. Sundar, K.V. Sharma, M.K. Singh, A.C.M. Sousa, *Hybrid nanofluids preparation, thermal properties, heat transfer and friction factor: A review.* Renewable and Sustainable Energy Reviews, 68(Part 1) (2017) 185-198.
[17]. R.J. Hunter, *Zeta Potential in Colloid Science: Principles and Applications.* Academic Press, New York, NY, USA 1981.
[18]. S. Bhattacharjee, *DLS and zeta potential: What they are and what they are not?* Journal of Controlled Release, 235 (2016) 337-351.
[19]. S. Honary, F. Zahir, *Effect of zeta potential on the properties of nano-drug delivery systems – a review (part 1),* Tropical Journal of Pharmaceutical Research, 12(2) (2013) 255-264.
[20]. T. Yoon, J. Kim, J. Kim, J.K. Lee, *Electrostatic self-assembly of Fe_3O_4 nanoparticles on graphene oxides for high-capacity lithium-ion battery anodes.* Energies, 6(9) (2013) 4830-4840.
[21]. Y. Zhang, B. Chen, L. Zhang, J. Huang, F. Chen, Z. Yang, J. Yao, Z. Zhang, *Controlled assembly of Fe_3O_4 magnetic nanoparticles on graphene oxide.* Nanoscale, 3(4) (2011) 1446-1450.
[22]. S. Bhattacharjee, C.H. Ko, M. Elimelech, DLVO interaction between rough surfaces. *Langmuir*, 14 (1998) 3365-3375.
[23]. P. Keblinski, J.A. Eastman, D.G. Cahill, Nanofluids for thermal transport. *Materials Today*, 8(6) (2005) 36-44.
[24]. J. Buongiorno, *Convective Transport in Nanofluids.* ASME Journal of Heat Transfer, 128(3) (2006) 240-250.
[25]. Y. Xuan, Q. Li, Heat transfer enhancement of nanofluids. *International Journal of Heat and Fluid Flow*, 21(1) (2000) 58-64.
[26]. W. Evans, J. Fish, P. Keblinski, *Role of Brownian motion hydrodynamics on nanofluid thermal conductivity.* Applied Physics Letters, 88 (2006) 093116.
[27]. J.N. Israelachvili, *Intermolecular and Surface Forces* (3rd ed.). 2011, Academic Press, New York, NY, USA.
[28]. W. Yu, S.U.S. Choi, *The role of interfacial layers in the enhanced thermal conductivity of nanofluids: A renovated Maxwell model.* Journal of Nanoparticle Research, 5 (2003) 167-171.
[29]. R. Prasher, P.E. Phelan, P. Bhattacharya, *Effect of aggregation kinetics on the thermal conductivity of nanoscale colloidal solutions (nanofluids).* Nano Letters, 6(7) (2006) 1529-1534.
[30]. C.W. Nan, G. Liu, Y. Lin, M. Li, Interface effect on thermal conductivity of carbon nanotube composites. *Applied Physics Letters*, 85 (2004) 3549-3551.
[31]. R.M. Mutiso, K.I. Winey, Electrical percolation in quasi-two-dimensional metal nanowire networks for transparent conductors. *Phys. Rev. E* 88 (2013) 032134.
[32]. J. Wensel, B. Wright, D. Thomas, W. Douglas, B. Mannhalter, W. Cross, H. Hong, J. Kellar, P. Smith, W. Roy, Enhanced thermal conductivity by aggregation in heat transfer nanofluids containing metal oxide nanoparticles and carbon nanotubes, Applied Physics Letters, 92 (2) (2008) 023110.
[33]. K. Maqsood, A. Ali, S.U. Ilyas, S. Garg, M. Danish, A. Abdulrahman, A.B. Mahfouz, S. Ridha, M. Mubashir, H.R. Lim, K.S. Khoo, P.L. Show, Multi-objective optimization of thermophysical properties of multiwalled carbon nanotubes based nanofluids, Chemosphere, 286 (2022) 131690.
[34]. M. Asadi, A. Asadi, S. Aberoumand, *An experimental and theoretical investigation on the effects of adding hybrid nanofluids on heat transfer efficiency and pumping power of an oil-based nanofluid as a coolant fluid.* International Journal of Refrigeration, 89 (2018) 83-92.
[35]. Z. Shah, A. Saeed, I. Khan, M.M. Selim, Ikramullah, P. Kumam, *Numerical modeling on hybrid nanofluid (Fe_3O_4 + MWCNT/H_2O) migration considering MHD effect over a porous cylinder.* PLoS ONE, 16(7) (2021) e0251744.
[36]. X-Q. Wang, A.S. Mujumdar, Heat Transfer Characteristics of Nanofluids: A Review. *International Journal of Thermal Sciences*, 46(1) (2007) 1-19.
[37]. A. Basu, A. Saha, S. Banerjee, P.C. Roy, B. Kundu, A review of artificial intelligence methods in predicting thermophysical properties of nanofluids for heat transfer applications. *Energies*, 17(6) (2024) 1351.
[38]. M.S. Abhijith, K.P. Soman, Machine learning methods for modeling nanofluid flows: a comprehensive review with emphasis on compact heat transfer devices for electronic device cooling, Journal of Thermal Analysis and Calorimetry, 149 (2024) 5843-5869.
[39]. L. Wang, H. Wang, D. Leng, S. Fang, Y. Yang, Y. Du, Machine learning applications in nanomaterials: recent advances and future perspectives, *Chemical Engineering Journal*, 500 (**2024**) 156687.

[40]. A. Agrawal, A. Choudhary, Perspective: materials informatics and big data: realization of the "fourth paradigm" of science in materials science. APL Materials, 4(5) (2016) 053208.
[41]. M. Raissi, P. Perdikaris, G.E Karniadakis, *Physics-informed neural networks: a deep learning framework for solving forward and inverse problems involving nonlinear partial differential equations. Journal of Computational Physics*, 378 (2019) 686-707.
[42]. F. Sahin, O. Genc, M. Gökcek, A.B. Çolak, From experimental data to predictions: artificial intelligence supported new mathematical approaches for estimating thermal conductivity, viscosity and zeta potential in Fe_3O_4-eater magnetic nanofluids, Power Technology, 430 (2023) 118974.
[43]. T. Lookman, P.V. Balachandran, D. Xue, R. Yuan, Active learning in materials science with emphasis on adaptive sampling using uncertainties for targeted design. NPJ Computational Materials, 5(2019) 21.
[44]. A. Jain, S.P. Ong, G. Hautier, W. Chen, W.D. Richards, S. Dacek, S. Cholia, D. Gunter, D. Skinner, G. Ceder, K.A. Persson, Commentary: the materials project: a materials genome approach to accelerating materials innovation, APL Materials, 1(1) (2013) 011002.
[45]. A. Sabeur, Machine Learning Applications in Nanofluid Research: A Comprehensive Review of Trends, Challenges, and Future Perspectives, in book: Applied Intelligence, editor V. Robles-Bykbaev, IntechOpen, London, UK, 2026.
[46]. National Academies of Sciences, Engineering, and Medicine; National Academy of Engineering, *Foundational Research Gaps and Future Directions for Digital Twins.* Washington DC: National Academies Press, 2024, March 28. Accessing on July 23, 2026 at Foundational Research Gaps and Future Directions for Digital Twins - PubMed.
[47]. F. Tao, Q. Qi, A. Liu, A. Kusiak, Data-driven smart manufacturing, Journal of Manufacturing Systems, 48, Part C (2018) 157-169.
[48]. S. Yin, T. Zhang, Y. Yu, X. Bu, Z. Zhang, J. Geng, X. Dong, H. Jiang, Study on the *preparation and optical properties of graphene oxide@Fe_3O_4 two-dimensional magnetically oriented nanocomposites.* Materials, 16(2) (2023) 476.
[49]. H. Ohshima, *Theory of Colloid and Interfacial Electric Phenomena*; Academic Press: Amsterdam, The Netherlands, 2006.
[50]. B.P. Binks, Particles as surfactants: Similarities and differences. *Current Opinion in Colloid & Interface Science*, 7(1-2) (2002) 21-41
[51]. B. Saleh, L.S. Sundar, *Thermal efficiency, heat transfer and friction factor analyses of MWCNT + Fe_3O_4/water hybrid nanofluids in a solar flat plate collector under thermosyphon condition,* Processes, 9(1) (2021) 180.
[52]. J.C. Maxwell, *A Treatise on Electricity and Magnetism*; Clarendon Press: Oxford, UK, 1873.
[53]. R.L. Hamilton, O.K. Crosser, Thermal conductivity of heterogeneous two-component systems. *Industrial & Engineering Chemistry Fundamentals,* 1(3) (1962**)** 187-191.
[54]. C.W. Nan, R. Birringer, D.R. Clarke, H. Gleiter, Effective thermal conductivity of particulate composites with interfacial thermal resistance. *J. Appl. Phys.* 81 (1997**)** 6692-6699.
[55]. W. Yu, H. Xie, X. Wang, X Wang, *Significant thermal conductivity enhancement for nanofluids containing graphene nanosheets.* Physics Letters A, 375(10) (2011) 1323-1328.
[56]. D.G. Cahill, W.K. Ford, K.E. Goodson, G.D. Mahan, A. Majumdar, H.J. Maris, R. Merlin, S.R. Philpot, Nanoscale thermal transport. *J. Appl. Phys.* 93 (2003**)** 793-818.
[57]. E.T. Swartz, R.O. Pohl, Thermal boundary resistance. *Rev. Mod. Phys.* 61 (1989**)** 605-668.
[58]. Z. Ge, D.G. Cahill, P.V. Braun, Thermal conductance of hydrophilic and hydrophobic interfaces. *Phys. Rev. Lett.* 96 (2006) 186101.
[59]. M. Bahiraei, S. Heshmatian, H. Hoayedi, Artificial intelligence in the field of nanofluids: a review on applications and potential future directions, *Powder Technology*, 353 (**2019**) 276-301.
[60]. T. Ma, Z. Guo, M. Lin, Q. Wang, Recent trends on nanofluid heat transfer machine learning research applied to renewable energy, *Renewable and Sustainable Energy Reviews*, 138 (**2021**) 110494.
[61]. E.J. Onyiriuka, Machine learning prediction of nanofluid thermal and flow characteristics, Ph.D. Dissertation of The University of Leeds, West Yorkshire, England, 2024.
[62]. M.A. Sadlq, An overview of artificial intelligence techniques for predicting thermophysical characteristics of nanofluids in heat transfer applications, *Journal of Thermal Analysis and Calorimetry*, 151 (**2026**) 12135-12153.
[63]. S.A. Jadidi, R. Moolya, R. Padidhapu, S. Subramanian, S. Moolya, From experiments to AI: a comparative

review of machine learning approaches for predicting nanofluid thermophysical properties, Nanomaterials, 16(4) (2026) 272.
[64]. J. Sarkar, P. Ghosh, A. Adil, A review on hybrid nanofluids: Recent research, development and applications. *Renew. Sustain. Energy Rev.* 43 (2015**)** 164-177.
[65]. C.E. Rasmussen, C.K.I. Williams, *Gaussian Processes for Machine Learning*; MIT Press: Cambridge, MA, USA, 2006.
[66]. C. Rudin, S*top explaining black box machine learning models for high stakes decisions and use interpretable models instead.* Nature Machine Intelligence, 1 (2019) 206-215.
[67]. C. Molnar, *Interpretable Machine Learning* (2nd ed.). Lulu Press, 2022.
[68]. B. Derjaguin, L. Landau, Theory of stability of strongly charged lyophobic sols and adhesion of strongly charged particles in solutions of electrolytes. Progress in Surface Science, 43(1) (1993) 30-59.
[69]. E.J.W. Verwey, J.T.G Overbeek, K. van Nes, *Theory of the Stability of Lyophobic Colloids*: The Interaction of Sol Particles Having an Electric Double Layer. 1948, digitized on February 6, 2017. Netherlands: Elsevier Publishing Company.
[70]. S.M. Lundberg, S.I. Lee, A unified approach to interpreting model predictions. *Advances in Neural Information Processing Systems* **2017**, *30*, 4765-4774.
[71]. K. Deb, *Multi-Objective Optimization Using Evolutionary Algorithms.* John Wiley & Sons, 2001.
[72]. C.A. Coello Coello, G.B. Lamont, D.A. Van Veldhuizen, *Evolutionary Algorithms for Solving Multi-Objective Problems* (2nd ed.), Springer, US, 2007.
[73]. P.D. Shima, J. Philip, B. Raj, *Magnetically controllable nanofluid with tunable thermal conductivity and viscosity.* Applied Physics Letters, 95 (2009) 133112.
[74]. K. Deb, A. Pratap, S. Agarwal, T. Meyarivan, A fast and elitist multiobjective genetic algorithm: NSGA-II. *IEEE Transactions on Evolutionary Computation* **2002**, *6*, 182-197.
[75]. X. Wang, L. Luo, J. Xiang, S. Zheng, S. Shittu, Z. Wang, X. Zhao, A comprehensive review on the application of nanofluid in heat pipe based on the machine learning: theory, application and prediction, *Renewable and Sustainable Energy Reviews*, 150 (**2021**) 111434.
[76]. K. Cacus, R. Buitrago-Sierra, B. Herrardo, E. Pabón, S.M.S. Murshed, Nanofluids' stability effects on the thermal performance of heat pipes, Journal of Thermal Analysis and Calorimetry, 136 (2019) 1597-1614.
[77]. S.M.S. Murshed, M. Sharifpur, S. Giwa, J.P. Meyer, Experimental research and development on the natural convection of suspensions of nanoparticles – a comprehensive review, Nanomaterials, 10(9) (2020) 1855.
[78]. L. Ward, A. Agrawal, A. Choudhary, C. Wolverton, A general-purpose machine learning framework for predicting properties of inorganic materials, NPJ Computational Materials, 2 (2016) 16028.
[79]. E. Stach, B. DeCost, A.G. Kusne, J. Hattrick-Simpers, K.A. Brown, K.G. Reyes, J. Schrier, S. Billinge, T. Buonassisi, I. Foster, C.P. Gomes, J.M. Gregoire, A. Mehta, J. Montoya, E. Olivetti, C. Park, E. Rotenberg, S.K. Saikin, S. Smullin, V. Stanev, B. Maruyama, Autonomous experimentation systems for materials development: a community perspective, Matter, 4(1) (2021) 2702-2726.
[80]. F. Häse, L.M. Roch, A Aspuru-Guzik, Next-generation experimentation with self-driving laboratories, Trends in Chemistry, 1(3) (2019) 282-291.
[81]. L. Breiman, Random forests. *Machine Learning* **2001**, *45*, 5-32.
[82]. MathWorks®. *Global Optimization Toolbox User's Guide: gamultiobj Function*. MathWorks, Natick, MA, USA.